

---

# Local Model Reconstruction Attacks in Federated Learning and their Uses

---

**Ilias Driouich**

ilias.driouich@inria.fr  
ilias.driouich@amadeus.com  
Inria, Univ. Côte d’Azur  
Amadeus

**Chuan Xu**

chuan.xu@inria.fr  
Univ. Côte d’Azur, Inria, CNRS, I3S

**Giovanni Neglia**

giovanni.neglia@inria.fr  
Inria, Univ. Côte d’Azur

**Frederic Giroire**

frederic.giroire@cnrs.fr  
Inria, Univ. Côte d’Azur, CNRS, I3S

**Eoin Thomas**

eoin.thomas@amadeus.com  
Amadeus

## Abstract

In this paper, we initiate the study of *local model reconstruction attacks* in the context of Federated Learning (FL). In this scenario, an honest-but-curious adversary eavesdrops on the messages exchanged between a client and the FL aggregator, and then reconstructs the model that the client would have independently trained, which we refer to as the local model. The local model potentially overfits the client’s local dataset and can subsequently serve as a potent springboard for initiating a variety of other privacy attacks, such as reconstructing specific samples in the client dataset, inferring sensitive attributes or identifying which client stores a specific sample. Our experiments demonstrate that this indirect approach—reconstructing the local model before launching attacks—achieves higher success rates compared to state-of-the-art attacks, both gradient-based and model-based ones, that seek to extract sensitive information directly from FL messages. Moreover, existing approaches often face severe performance degradation when factors such as the size of the client’s local dataset, the gradient batch size or the number of local gradient updates increase, potentially limiting their effectiveness in real-world scenarios. Conversely, attacks initiated on a reconstructed local model demonstrate remarkable resilience to these variables, potentially posing a more formidable threat to user privacy.

## 1 Introduction

Federated Learning (FL) [1–3] is a distributed machine learning strategy in which multiple devices, also known as clients, work collaboratively to train a shared model. This process, orchestrated by a central server, allows data to remain locally on each device, thereby potentially enhancing data privacy. However, recent research has indicated that an honest-but-curious adversary—e.g., the server itself—can deduce sensitive client information simply by eavesdropping on the communication exchanges between a client and the server.

Privacy attacks under an honest-but-curious adversary in the FL environment can be broadly categorized into two types: gradient-based and model-based attacks.

In the first case, the adversary works with the client’s pseudo-gradients, that is the difference between the model the client receives from the server and the model returned by the client [4].<sup>1</sup> By leveraging the pseudo-gradients (hereafter simply called gradients), the adversary can reconstruct private training samples (e.g., images) as demonstrated by [5–9]. This type of exploit is referred to as the *sample reconstruction attack* (SRA). However, this attack may have limited impact, especially when clients employ large batch sizes and execute multiple local gradient updates (a practice that is commonly employed to minimize communication overhead). For instance, as per [8, Table 6a], the SRA success rate on the LFW dataset drops from 100% to 13% as the batch size increases from 1 to 16, and from 100% to 39% when the number of local steps rises from 1 to 9. Similarly, [9, Figure 8] reports a decrease from 100% to 28% on the ImageNet dataset as the batch size grows from 1 to 48. Commenting on similar results, [10] recommends the use of larger batch sizes as a potential mitigation strategy against the SRA.

Leaked gradients in FL may also lead to an *attribute inference attack* (AIA) [11], provided the adversary has access to the public attributes of the victim’s dataset. However, as this attack attempts to infer per-sample private attribute values while gradients combine information from multiple samples, its effectiveness is significantly diminished with larger datasets. Notably, the attack accuracy almost halves on the Genome dataset when the size of the client’s local dataset increases from 50 to 1000 samples [11, Table 9].

Alternatively, the adversary could directly exploit the global model or the client’s updated model to glean private information about the client. Model-based versions of previously discussed SRA and AIA have been proposed in studies like [12] and [13–15], respectively; a model-based Source Inference Attack (SIA) has been proposed in [16].

However, the effectiveness of model-based attacks typically relies on the model overfitting the client’s local data, which is generally not the case for models exchanged between the clients and the server in Federated Learning. Indeed, the shared model disseminated by the server at any communication round is an aggregate of models from numerous clients and can significantly differ from the model that a client would independently learn [17, Figures 2,3]. Consequently, direct attacks on the global model may offer limited value.

The updated model from the client could potentially serve as a more viable target for a direct attack. However, Federated Learning systems are typically configured to mitigate overfitting by the client—for instance, by limiting the number of local gradient steps. This approach is critical as client overfitting could obstruct the convergence of the global model, especially considering the diversity inherent in clients’ local datasets [1, 18].

In this paper, we introduce a novel threat called the *local model reconstruction attack* (LMRA). In this scenario, an adversary, such as a curious server, aims to reconstruct the model that a client would have trained exclusively on its local dataset. This type of attack poses a significant risk as it allows the adversary to launch the aforementioned model-based attacks with heightened efficiency. For instance, the adversary could successfully reconstruct private facial images utilized during the FL training with a batch size of 32, a task on which existing gradient-based SRAs fail and, existing naive model-based SRAs perform much worse (refer to Figure 1).

Our main contributions can be summarized as follows:

- We propose a new attack, the local model reconstruction attacks for FL. The attack works for *any machine learning model*, e.g., neural network regression/classification, using the heuristic presented in Sec. 3.2. We further provide theoretical guarantees on the attack success for a linear regression model (Sec. 3.1).
- Empirical results using realistic datasets confirm that our LMRA works well on both regression and classification tasks and that it is less sensitive to the batch size, the number of local steps, and the local dataset size. Furthermore, we show how the decoded local model obtained from LMRA may be leveraged to initiate several known attacks (e.g., SRA, AIA, and SIA) with performances surpassing that of the state-of-the-art attacks (Sec. 4).

---

<sup>1</sup>The pseudo-gradient is proportional to the gradient when the client performs a single gradient step.

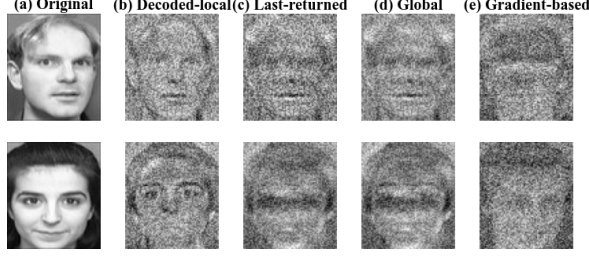


Figure 1: Sample reconstruction attacks (SRA): Images recovered when training a neural network model on AT&T facial dataset [19] among 10 clients through FedAvg under batch size 32 and 1 local epoch. The honest-but-curious adversary can inspect the raw messages exchanged between the server and the client. Images (b), (c), and (d) are reconstructed by the model-based SRA [12] on our decoded local model, the last-returned model from the attacked client, and the global model, respectively. Image (e) is obtained by the well-known gradient-based SRA [7].

## 2 Preliminaries

### 2.1 Federated learning

We denote by  $\mathcal{C}$  the set of all clients participating to FL. Let  $\mathcal{D}_c = \{(\mathbf{x}_c(i), y_c(i)), i = 1, \dots, S_c\}$  be the local dataset of client  $c \in \mathcal{C}$  and  $S_c$  denote the size of  $\mathcal{D}_c$ . Each data sample  $(\mathbf{x}_c(i), y_c(i))$  is a pair consisting of an input  $\mathbf{x}_c(i)$  and of an associated target value  $y_c(i)$ . In FL, clients cooperate to learn a global model, which minimizes the following empirical risk over all the data owned by clients:

$$\min_{\theta \in \mathbb{R}^d} \mathcal{L}(\theta) = \sum_{c \in \mathcal{C}} p_c \mathcal{L}_c(\theta, \mathcal{D}_c) = \sum_{c \in \mathcal{C}} p_c \left( \frac{1}{S_c} \sum_{i=1}^{S_c} l(\theta, \mathbf{x}_c(i), y_c(i)) \right), \quad (1)$$

where  $l(\theta, \mathbf{x}_c(i), y_c(i))$  measures the loss of the model  $\theta$  on the sample  $(\mathbf{x}_c(i), y_c(i)) \in \mathcal{D}_c$  and  $p_c$  is the positive weight of client  $c$ , s.t.,  $\sum_{c \in \mathcal{C}} p_c = 1$ . Common choices of weights are  $p_c = \frac{1}{|\mathcal{C}|}$  or  $p_c = \frac{S_c}{\sum_{c \in \mathcal{C}} S_c}$ .

---

#### Algorithm 1 FL Framework

---

**Output:**  $\theta(T)$

Server  $s$ :

- 1: **for**  $t \in \{0, \dots, T - 1\}$  **do**
- 2:    $s$  selects a subset of the clients  $\mathcal{C}_s(t) \subseteq \mathcal{C}$ ,
- 3:    $s$  broadcasts the global model  $\theta(t)$  to  $\mathcal{C}_s(t)$ ,
- 4:    $s$  waits for the updated models  $\theta_c(t)$  from every client  $c \in \mathcal{C}_s(t)$ ,
- 5:    $s$  computes  $\theta(t + 1)$  by aggregating the received updated models.

Client  $c \in \mathcal{C}$ : Input  $\theta$ , Output  $\theta_c$

- 6: **while** FL training is not completed **do**
  - 7:    $c$  listens for the arrival of new global model  $\theta$ ,
  - 8:    $c$  updates its model  $\theta_c$  based on  $\theta$  and  $\mathcal{D}_c$ ,
  - 9:    $c$  sends back  $\theta_c$  to the server.
- 

averaged with constant weights, and the clients perform locally multiple stochastic gradient steps (Appendix A).

### 2.2 Threat Model

We consider an honest-but-curious adversary<sup>2</sup>, which is a standard threat model in FL [23, Table 7] and is commonly considered in existing literature [24, 7–9, 25, 11, 16]. This adversary is knowledgeable about the trained model structure, the loss function, and the training algorithm, and may eavesdrop on communication between the attacked client and the server but does not interfere with the training

<sup>2</sup>In what follows, we refer to the client using female pronouns and the adversary using male pronouns, respectively.

process.<sup>3</sup> For instance, during training round  $t$ , the adversary can inspect the messages exchanged between the server and the attacked client (denoted by  $c$ ), allowing him to recover the parameters of the global model  $\theta(t)$  and the updated client model  $\theta_c(t)$  (Algorithm 1). It is worth noting that the FL server itself could act as the adversary.

When it comes to defenses against such an adversary, it is crucial to understand that traditional measures like encrypted communications are ineffective against the FL server. Although more sophisticated cryptographic techniques like secure aggregation protocols [26, 27] (which allow the server to aggregate local updates without having access to each individual update) do hide the client updated model  $\theta_c(t)$  from the server, they come with a significant computation overhead [28] and are inefficient for sparse vector aggregation [23]. Moreover, these techniques can be vulnerable to poisoning attacks, as they hinder the server from detecting (and removing) potentially harmful updates from malicious clients [29–31]. For instance, [32, Sec. 4.4] introduces a new class of data poisoning attacks that succeed when training models with secure multiparty computation. Alternatively, Trusted Execution Environments (TEEs) [33, 34], which provide an encrypted memory region to ensure the code has been executed faithfully and privately, can both conceal clients’ updated models and defend against poisoning attacks. However, implementing a reliable TEE platform in FL remains an open challenge due to the infrastructure resource constraints and the required communication processes needed to connect verified codes [23].

In the subsequent section, we provide an overview of several well-known attacks targeting FL systems. The local model reconstruction attack proposed in this paper can be used by an honest-but-curious adversary as a preliminary step to execute these attacks.

### 2.3 Attacks in FL under honest-but-curious adversary

Let  $\mathcal{T}_c \subseteq \{t | c \in \mathcal{C}_s(t), \forall t \in 0, \dots, T - 1\}$  denote the set of communication rounds during which the adversary inspects messages exchanged between the server and the attacked client and  $\mathcal{M}_c = \{(\theta(t), \theta_c(t)), \forall t \in \mathcal{T}_c\}$  denote the corresponding set of messages. Furthermore, let  $\theta_c^* = \arg \min_{\theta \in \mathbb{R}^d} \mathcal{L}_c(\theta, \mathcal{D}_c)$  be the optimal local model for client  $c$ .

**Source inference attack (SIA)** SIA aims to identify the source of a particular training record  $(\mathbf{x}_c, y)$ , i.e., the originating FL client [16]. Uncovering the source may reveal sensitive information, such as the hospital where a patient was treated. Specifically, the attack proposed in [16] identifies the most likely source as the client whose updated model exhibits the smallest loss on the record  $(\mathbf{x}_c, y)$ . The proposed SIA method shows a higher success rate as the updated machine learning model increasingly overfits the local dataset [16, Fig. 2]. This finding suggests that the best candidate for carrying out the attack could potentially be the optimal local model.

**Attribute inference attack (AIA)** AIA leverages public information to deduce private or sensitive attributes [13, 11, 14, 15]. For example, an AIA could reconstruct a user’s gender from a recommender model by having access to the user’s provided ratings. Formally, each input  $\mathbf{x}_c(i)$  consists of public attributes  $\mathbf{x}_c^p(i)$  and a sensitive attribute  $s_c(i)$ . The target value, assumed to be public, is denoted by  $y_c^p(i)$ . The adversary, having access to  $\{(\mathbf{x}_c^p(i), y_c^p(i)), i = 1, \dots, S_c\}$  and  $\mathcal{M}_c$ , aims to recover the sensitive attributes  $s_c(i)$  [13, 11].<sup>4</sup>

The reference [11] presents a *gradient-based* AIA specifically designed for the FL context. The central idea involves identifying sensitive attribute values that yield virtual gradients closely resembling the client’s model updates (referred to as pseudogradients), in terms of cosine similarity. Formally, the adversary solves the following optimization problem:

$$\arg \max_{\{s_c(i)\}_{i=1}^{S_c}} \sum_{t \in \mathcal{T}_c} \text{cosineSim} \left( \frac{\partial \mathcal{L}_c(\theta(t), \{(\mathbf{x}_c^p(i), s_c(i), y_c^p(i)), i = 1, \dots, S_c\})}{\partial \theta(t)}, \theta(t) - \theta_c(t) \right). \quad (2)$$

From Equation (2), we observe that, since gradients incorporate information from all samples, the attack performance deteriorates in the presence of a large local dataset, as evidenced by the experiments in [11].

<sup>3</sup>The attribute inference attack (see Sec. 2.3) assumes that the honest-but-curious adversary has also access to public features of samples at client  $c$ .

<sup>4</sup>In [14, 15], the adversary possesses additional information, including estimates of the marginals or the joint distribution of the data samples. However, in this paper, we do not consider such a more powerful adversary.

As an alternative, the AIA can be executed directly on the model (rather than on the model pseudogradients), as initially proposed for the centralized setting in [13]. Let  $\mathbf{h}_\theta$  denote the output of model  $\theta$ , i.e., a real number for a regression task and a probability distribution for a classification task. Given a released ML model  $\theta$ , the adversary can infer the sensitive attributes by solving the following optimization problem:

$$\operatorname{argmin}_{s_c(i)} \|\mathbf{h}_\theta(\mathbf{x}_c^p(i), s_c(i)) - y_c^p(i)\|_2^2, \quad \forall i \in \{1, \dots, S_c\}, \quad (3)$$

where  $y_c^p(i)$  is a real number or a label one-hot-encoding for regression and classification, respectively.

We provide theoretical guarantees (Appendix B.1) for the accuracy of the model-based AIA attack (Problem (3)) to least squares regression when FL clients compute full batch gradients. In particular, we show that, if the model  $\theta$  fits well the local data or if the sensitive attribute has significant importance on the final prediction, the attack can achieve almost 100% accuracy. This result suggests that AIA on models do not suffer the limit of AIA on gradients, namely their sensitivity to the dataset size. Furthermore, our theoretical finding motivates the adversary to trigger AIA on a model as close as possible to the optimal local model, which is more likely to overfit the local dataset.

**Sample reconstruction attack (SRA)** The SRA pushes the AIA approach even further as it aims to reconstruct the entire private training dataset from the gradients [5–10] or from the model [12]. For instance, in the FL context, a well-known gradient-based SRA proposed in [7] reconstructs the  $B$  images in the client’s batch used at each round  $t \in \mathcal{T}_c$ . This is achieved by solving the following optimization problem:

$$\operatorname{argmax}_{\{\mathbf{x}(i), y(i)\}_{i=1}^B} \operatorname{cosineSim} \left( \frac{\partial \mathcal{L}_c(\theta(t), \{\mathbf{x}(i), y(i), i = 1, \dots, B\})}{\partial \theta(t)}, \theta(t) - \theta_c(t) \right) - \alpha \sum_{i=1}^B TV(\mathbf{x}(i)), \quad (4)$$

where the image total variation [35] is used as a regularization term. This attack is effective only when gradients are calculated on extremely small batches [8, 10] when the number of gradient steps is small [8] or when the adversary knows the BatchNorm statistics of the private batch [10].<sup>5</sup>

Alternatively, the SRA can be executed directly on the model for classification [12]. For example, the adversary can reconstruct one training sample for each of the  $K$  classes by solving the  $K$  optimization problems:

$$\operatorname{argmax}_{\mathbf{x}(k)} \mathbf{h}_\theta(\mathbf{x}(k))[k], \quad \forall k \in \{1, \dots, K\}. \quad (5)$$

The model-based version of SRA is likely less sensitive to batch size and more sensitive to the model fit to the data.

### 3 Local Model Reconstruction Attack

In this section, we show how an honest-but-curious adversary (Sec. 2.2) may reconstruct the optimal local model of client  $c$ , i.e.,  $\theta_c^* = \arg \min_{\theta \in \mathbb{R}^d} \mathcal{L}_c(\theta, \mathcal{D}_c)$ .

First, we prove theoretical results for linear models, showing that the adversary can perfectly reconstruct the optimal local model under deterministic FL updates and provide guarantees on the reconstruction error under stochastic FL updates (Sec. 3.1). Second, we propose a heuristic to perform the local model reconstruction attack for any machine learning model trained in a federated way (Sec. 3.2).

#### 3.1 Guarantees for Linear Model Reconstruction

We consider that clients cooperatively train a linear regression model with quadratic loss. We refer to this setting as a federated least squares regression. Remember that a client’s design matrix has a number of rows equal to the input features of the samples in the client’s local training dataset.

We first show that the adversary can exactly reconstruct the optimal local model if the attacked client performs full-batch gradient updates, as it may be the case with the popular FedAvg algorithm [1].

<sup>5</sup>It is worth noting that FL training can be performed without sharing BatchNorm statistics between the clients and the server [36].

**Proposition 1.** Consider a federated least squares regression and assume that client  $c$  has  $d$ -rank design matrix and updates the global model through full-batch gradient updates. Once the adversary eavesdrops  $d + 1$  communication exchanges between client  $c$  and the server, it can recover the client’s optimal local model by solving  $d$  linear systems with  $d + 1$  variables, and then with  $O(d^4)$  operations.

The reconstruction procedure is detailed in the proof of Proposition 1 in Appendix B.2. We remark that the result holds independently of the number of local gradient updates performed by the client at each round.

The following proposition shows that the attack in Proposition 1 is order-optimal in terms of the number of messages the adversary needs to eavesdrop. The proof is moved to Appendix B.3.

**Proposition 2.** Consider that FedAvg with one local step is employed for a federated least squares regression. At least one client is required to communicate with the server  $\Omega(d)$  times for the global model to be learned, and the adversary needs to eavesdrop at least  $\Omega(d)$  messages from this client to reconstruct her optimal local model.

If the attacked client’s updates are random, e.g., due to batch sampling, the adversary can still reconstruct the client’s optimal local model with high probability.

**Proposition 3 (Informal statement).** Consider a federated least squares regression with a large number of clients and assume that client  $c$  has  $d$ -rank design matrix, that she updates the global model through stochastic gradient steps with sub-Gaussian noise with scale  $\sigma$  and small learning rate  $\eta$ , and that global models are heterogeneous. By eavesdropping on  $n_c > d$  message exchanges between client  $c$  and the server, the adversary can reconstruct the optimal local model, denoted by  $\hat{\theta}_c^*$ , with error:

$$\left\| \theta_c^* - \hat{\theta}_c^* \right\|_2 \leq \mathcal{O} \left( \eta \sigma d (\|\theta_c^*\|_2 + 1) \sqrt{\frac{d + 1 + \ln \frac{2}{\delta}}{n_c}} \right), \quad \text{w.p.} \geq 1 - \delta, \quad (6)$$

by solving  $d$  least squares problems with  $d + 1$  variables and  $\frac{n_c}{d}$  points, and then with  $O(n_c d^2)$  operations.

The formal statement of Proposition 3 and its proof are in Appendix B.4.

### 3.2 Heuristic for Local Model Reconstruction

In this section, we present a heuristic for local model reconstruction attacks (Algorithm 2) applicable to any machine learning models trained using a Federated Learning algorithm that conforms to the framework described in Algorithm 1.

---

**Algorithm 2** Local model reconstruction attack

---

**Input:**  $\mathcal{M}_c = \{(\theta(t), \theta_c(t)), \forall t \in \mathcal{T}_c\}$ , the messages inspected by the adversary.

- 1:  $\Delta \mathcal{M}_c = \{(\theta, \Delta \theta = \theta_c - \theta), \forall (\theta, \theta_c) \in \mathcal{M}_c\}$
- 2: Define a mapping function  $\mathcal{G}_c : \mathbb{R}^m \times \mathbb{R}^d \rightarrow \mathbb{R}^d$  with parameters  $w \in \mathbb{R}^m$ , taking the server model  $\theta \in \mathbb{R}^d$  as input and predicting the local update, i.e., the difference between the local model and the server model.
- 3: Estimate  $\mathcal{G}_c$  parameters, by minimizing the empirical risk:

$$\hat{w} = \arg \min_{w \in \mathbb{R}^m} \sum_{(\theta, \Delta \theta) \in \Delta \mathcal{M}_c} \|\mathcal{G}_c(w, \theta) - \Delta \theta\|^2 \quad (7)$$

- 4: Estimate the model  $\hat{\theta}_c$ , by minimizing the norm of the local update  $\mathcal{G}_c$  for fixed parameters  $\hat{w}$ :

$$\hat{\theta}_c = \min_{\theta \in \mathbb{R}^d} \|\mathcal{G}_c(\hat{w}, \theta)\|^2 \quad (8)$$

- 5: Return  $\hat{\theta}_c$  as the estimator for the local model of client  $c$
- 

Our approach for approximately reconstructing the local model of client  $c$  consists of two steps. First, the adversary learns a mapping function  $\mathcal{G}_c(\hat{w}, \cdot)$  to mimic the local update rule of the client

by examining the messages in  $\mathcal{M}_c$  (see (7) in Algorithm 2). Specifically, given the server model  $\theta$  as input,  $\mathcal{G}_c(\hat{w}, \theta)$  predicts the client’s update  $\Delta\theta = \theta_c - \theta$ . Second, the adversary estimates the local model of client  $c$  as the one that minimizes  $\|\mathcal{G}_c(\hat{w}, \theta)\|^2$  (see (8) in Algorithm 2). The intuition behind this step is that the client would not update the server model ( $\Delta\theta = 0$ ) if it coincides with its optimal local model.

When executing FedAvg using a full batch size, the exact mapping function  $\mathcal{G}_c$  can be accurately estimated for least squares regression and is shown to be linear (see (15) in Appendix B.2). In this case, minimizing  $\|\mathcal{G}_c\|^2$  corresponds to solving the linear systems mentioned in Proposition 1. Therefore, the decoding algorithm in Proposition 1 can be viewed as a specific instance of Algorithm 2, which, in particular, results in the correct reconstruction of the optimal local model, as proven above.

In general, the performance of our heuristic relies on two factors: 1) the effectiveness of the mapping function  $\mathcal{G}_c$  in mimicking the specific client’s update rule (Algorithm 1, line 8), and 2) the proximity of the estimated  $\hat{\theta}$  to the true minimizer of Problem (8) when  $\|\mathcal{G}_c\|^2$  is non-convex.

The first factor depends on the complexity of the learning task, the complexity of the mapping function, the randomness introduced by the client’s update rule, and the number of messages observed by the adversary. In particular, the more randomness introduced, the less accurate the estimation of  $\mathcal{G}_c$ , and consequently, the reconstructed local model. Privacy defenses that amplify the randomness in the original algorithm, such as adding noise [37], sub-sampling [38, 39], or randomly combining data samples [40, 41], are expected to affect the performance of our local model reconstruction attack. In Section D.4, we show that this is indeed the case, but, *even in presence of such privacy defenses, SIA, AIA, and SRA attacks triggered on top of the local model reconstruction attack outperform state-of-the-art attacks*. In presence of noisy updates, the more messages the adversary can inspect, the closer  $\mathcal{G}_c$  will resemble the local update rule, resulting in a smaller model reconstruction error (as shown in Proposition 3 for the federated least squares regression). At the same time, our experimental results suggest that an adversary can reconstruct a neural network model by eavesdropping on merely 10% of the messages exchanged between the client and the server throughout the entire training process. This number of messages is notably smaller than what one might expect based on the theoretical results (Propositions 1 and 3). Note that one-shot FL algorithms may seem to contrast our attack, but they might release directly the optimal local model [42, 43].

The second factor is influenced by the structure of  $\mathcal{G}_c$ . Experiments in the next section demonstrate that our heuristic exhibits strong performance even when  $\mathcal{G}_c$  is implemented as a neural network, which results in a highly non-convex Problem (8).

## 4 Experiments

**Datasets and model** We consider four datasets: Flight Prices for the regression task, Adult [44], Leaf Synthetic [45], and AT&T dataset [19] for the classification tasks. Flight Prices includes flight ticket information for the 10 largest European airlines. Adult contains records with individuals’ information such as sex, age, education level; it is a popular benchmark in ML for studying inference attacks and privacy [46, Tables 2–4][47, 32]. Leaf Synthetic is a common benchmark for federated learning. The AT&T dataset contains facial images for 40 different persons and has been considered in many privacy leakage studies [12, 48–50]. For all tasks, the model is a fully-connected 3-layer neural network. We train it also with batch normalization (BN) to show its effect on FL attacks [10]. Appendix C.1 provides more detailed information about these datasets and the model.

**Attacks** We execute four attacks on every client involved in the FL training: *Local Model Reconstruction Attack* (LMRA), *Attribute Inference Attack* (AIA), *Sample Reconstruction Attack* (SRA), and *Source Inference Attack* (SIA).<sup>6</sup> The model is trained through FedAvg [1] for a total number of 1000 communication rounds. The adversary inspects only 100 communication rounds. Other FL hyperparameters, attacks parameters and implementation details can be found in Appendix C.2.

**Evaluation Metrics** We show the average attack performance over all the clients. For LMRA, we measure the distance between the tested model and the client’s optimal local model using the recent

<sup>6</sup>Since AIA targets tabular dataset and SRA targets image dataset, we run AIA on Flight Prices, Adult, and Leaf Synthetic, and SRA on AT&T.

approach Zest [51]. Zest is architecture-independent and computes the cosine similarity between the explanations obtained by LIME [52] for the two models (the higher the value, the more similar to two models). For AIA, the sensitive attributes are the journey type for Flight Prices, the gender for Adult, and one synthetic binary attribute for Leaf Synthetic. The accuracy of AIA is the fraction of correctly reconstructed attributes. For SRA, we measure the quality of the reconstructed image w.r.t. the original one using the Structural Similarity Index Measure (SSIM) [53]. SIA’s accuracy is the fraction of target records for which the source has been correctly identified.

**Baselines** For LMRA, there is no state-of-the-art (SOTA) method to compare with, but the adversary could use the global model or the client’s last-returned model as proxies for the local model. We compare LMRA-enabled AIA and SRA with the most recent gradient-based AIA [11] and the well-known SRA [7] methods, corresponding to (2) and (4), respectively. For SIA, we compare our LMRA-enabled approach with the SOTA attack proposed in the original work [16] that chooses as source the client whose updated model exhibits the smallest loss on the training record. We trigger the AIA, SRA, and SIA attacks not only on the local model reconstructed from LMRA, but also on its potential proxies: the global model or the last-returned model.

#### 4.1 Experimental results

Table 1 summarizes the performances of the four attacks when the neural network is trained with and without batch normalization. First, we observe that the local model reconstructed by LMRA is closer to the optimal local model than the global model and the last-returned model.<sup>7</sup> Second, AIA, SRA, and SIA performed on the LMRA reconstructed models consistently outperform the baselines. Third, although batch normalization makes all the attacks less effective as observed in [10], LMRA-based attacks still outperform all the baselines.

Attack	Metric	Dataset	Without BN				With BN			
			SOTA	Global	Last-returned	Ours	SOTA	Global	Last-returned	Ours
LMRA	Zest (%)	Flight Prices	-	71.4	70.7	<b>84.2</b>	-	61.5	63.3	<b>79.1</b>
		Adult	-	70.7	68.6	<b>88.4</b>	-	63.2	61.5	<b>83.4</b>
		Leaf Synthetic	-	67.3	65.3	<b>78.2</b>	-	60.7	60.1	<b>74.5</b>
		AT&T	-	52.8	55.2	<b>57.3</b>	-	50.2	51.6	<b>55.9</b>
AIA	Accuracy (%)	Flight Prices	73.1	70.7	70.2	<b>77.8</b>	71.9	70.3	68.6	<b>74.2</b>
		Adult	67.6	61.3	62.1	<b>73.1</b>	64.1	60.1	59.6	<b>70.6</b>
		Leaf Synthetic	66.3	61.1	60.6	<b>71.1</b>	62.9	56.1	57.8	<b>68.9</b>
SRA	SSIM (%)	AT&T	26.1	25.5	24.3	<b>34.3</b>	24.1	23.6	23.7	<b>33.2</b>
SIA	Accuracy (%)	Flight Prices	82.1	-	64.4	<b>84.3</b>	80.7	-	59.7	<b>81.3</b>
		Adult	77.6	-	61.0	<b>79.4</b>	75.1	-	60.5	<b>78.6</b>
		Leaf Synthetic	77.4	-	61.4	<b>79.3</b>	74.6	-	59.3	<b>77.9</b>
		AT&T	58.9	-	52.3	<b>63.8</b>	57.1	-	50.8	<b>61.6</b>

Table 1: The performance of local model reconstruction attack (LMRA), attribute inference attack (AIA), sample reconstruction attack (SRA), and source inference attack (SIA) when training a neural network w/wo batch normalization (BN) with 1 local epoch and batch size 512 (32 for AT&T dataset).

As discussed in Sec. 2.3, gradient-based AIA [11] and SRA [7] are sensitive to the local dataset size and the batch size/local epochs, respectively. In the following, we investigate the sensitivity of the alternative model-based attacks.

**Impact of the local dataset size on AIA.** In Figure 2, we show that the average accuracy (indicated by the green triangles) for SOTA drops from 0.76 to 0.62 for Flight Prices, from 0.77 to 0.61 for Adult, and from 0.73 to 0.58 for Leaf Synthetic. This result is expected as SOTA gradient-based AIA suffers from large datasets (see Sec. 2.3). On the contrary, our AIA shows stable performance. As a result, its performance advantage over SOTA increases as the dataset size increases.

<sup>7</sup>The performance of the global/last-returned/optimal local/reconstructed models on the training dataset can be found in Appendix D.1.

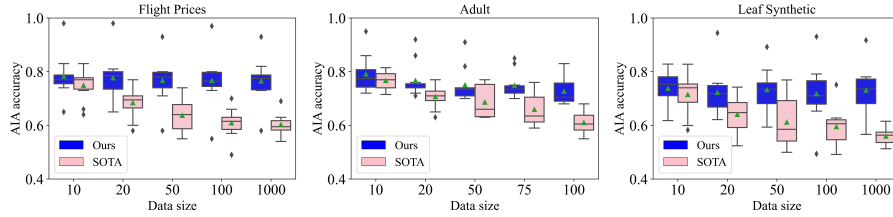


Figure 2: Influence of the local dataset size on the AIA accuracy when training a neural network wo BN with 1 epoch and batch size equal to the minimum between 256 and the client’s local dataset size. The green triangles represent the average accuracy over all clients and the bars represent the median.

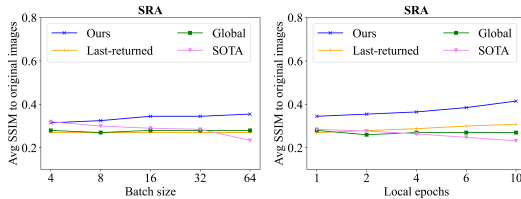


Figure 3: Batch size/Local epochs effect on SRA when training a neural network wo BN on AT&T. Default values for the number of local epochs and the batch size are 1 and 32, respectively.

provides the examples of reconstructed images for the batches with 64 samples. This demonstrates that using a large batch size *is not* a way to weaken SRA for model-based attacks.<sup>8</sup> The impact of batch size and local epochs on other attacks is evaluated in Appendix D.3.

**Impact of batch size and the number of local epochs on SRA.** Figure 3 shows that the model-based SRAs are less sensitive to the batch size and to the number of local epochs than the SOTA attack and ours outperform all the baselines in all settings, except for very small batch sizes for which it achieves similar reconstructed image quality. As the batch size or the number of local epochs increases, the performance of our attack is maintained or even improves, whereas the performance of SOTA drops by 9.2 and 5.1 p.p., respectively. Appendix D.2 provides the examples of reconstructed images for the batches with 64 samples. This demonstrates that using a large batch size *is not* a way to weaken SRA for model-based attacks.<sup>8</sup> The impact of batch size and local epochs on other attacks is evaluated in Appendix D.3.

**Impact of the number of clients.** The previous experiments are conducted in an FL system with 10 clients. Here, we investigate how its scale influences the performance of the attacks. First, note that our theoretical results show that the success of LMRA (Propositions 1 and 3) and model-based AIA (Proposition 4) does not depend on the total number of clients participating in FL, at least for a federated least squares regression. For neural networks, we carried out experiments with 10 to 100 clients for LMRA, AIA, and SIA on Leaf Synthetic and 10 to 40 clients for SRA on AT&T. Results are reported in Figure 4. As expected, we observe a small decrease of SIA efficiency with the number of potential sources. We also note a similar behavior for AIA SOTA. However, overall, the scale of the FL system has a limited impact on the attack performance.

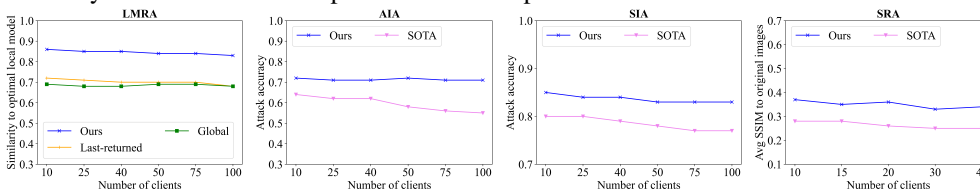


Figure 4: Impact of the number of clients on the attack efficiency when training a neural network wo BN on Leaf Synthetic for LMRA, AIA, SIA and on AT&T for SRA. The number of local epochs/batch size are set to 1/512 for Leaf Synthetic dataset and 1/32 for AT&T dataset, respectively.

**Impact of defense mechanisms** In Appendix D.4, we evaluate to what extent some known defenses, namely Differential Privacy [54] and Mixup [40], are able to mitigate the attacks. Our experiments show that even under these defense mechanisms our LMRA-based attacks outperform the baselines.

## 5 Conclusion

In this paper, we initiate the study of a new attack for FL: the adversary reconstructs a client’s optimal local model, and then use the reconstructed model to launch known model-based attacks with high success rate. This local model reconstruction attack does not suffer from a large number of local

<sup>8</sup>Note that, in [10, Sec. 6], the authors suggest to use large batch sizes to weaken SRA.

epochs, from large batch sizes, or from large dataset size, where the gradient-based attacks in the literature do. Thus, our work provides a new angle for designing powerful attacks for FL. These improved attacks might be used by curious users to discover private information. We hope to raise awareness that more research should be done to assess the privacy risk in FL and to propose efficient defense mechanisms.

## References

- [1] Brendan McMahan, Eider Moore, Daniel Ramage, Seth Hampson, and Blaise Aguera y Arcas. Communication-efficient learning of deep networks from decentralized data. In *Artificial Intelligence and Statistics*, pages 1273–1282. PMLR, 2017.
- [2] Xiangru Lian, Ce Zhang, Huan Zhang, Cho-Jui Hsieh, Wei Zhang, and Ji Liu. Can decentralized algorithms outperform centralized algorithms? A case study for decentralized parallel stochastic gradient descent. In *Advances in Neural Information Processing Systems 30: Annual Conference on Neural Information Processing Systems 2017*, pages 5330–5340, 2017.
- [3] Tian Li, Anit Kumar Sahu, Manzil Zaheer, Maziar Sanjabi, Ameet Talwalkar, and Virginia Smith. Federated optimization in heterogeneous networks. *MLSys*, 2020.
- [4] Martin Schechter. *Critical points*, page 45–86. Cambridge Studies in Advanced Mathematics. Cambridge University Press, 2005.
- [5] Ligeng Zhu, Zhijian Liu, and Song Han. Deep leakage from gradients. In *Advances in Neural Information Processing Systems*, pages 14774–14784, 2019.
- [6] Bo Zhao, Konda Reddy Mopuri, and Hakan Bilen. idlg: Improved deep leakage from gradients. *CoRR*, abs/2001.02610, 2020.
- [7] Jonas Geiping, Hartmut Bauermeister, Hannah Dröge, and Michael Moeller. Inverting gradients - how easy is it to break privacy in federated learning? In Hugo Larochelle, Marc’Aurelio Ranzato, Raia Hadsell, Maria-Florina Balcan, and Hsuan-Tien Lin, editors, *Advances in Neural Information Processing Systems 33: Annual Conference on Neural Information Processing Systems 2020, NeurIPS 2020, December 6-12, 2020, virtual*, 2020.
- [8] Wenqi Wei, Ling Liu, Margaret Loper, Ka-Ho Chow, Mehmet Emre Gursay, Stacey Truex, and Yanzhao Wu. A framework for evaluating client privacy leakages in federated learning. In *Computer Security – ESORICS 2020: 25th European Symposium on Research in Computer Security, ESORICS 2020, Guildford, UK, September 14–18, 2020, Proceedings, Part I*, page 545–566, Berlin, Heidelberg, 2020. Springer-Verlag.
- [9] Hongxu Yin, Arun Mallya, Arash Vahdat, Jose M Alvarez, Jan Kautz, and Pavlo Molchanov. See through gradients: Image batch recovery via gradinversion. In *Proceedings of the IEEE/CVF Conference on Computer Vision and Pattern Recognition*, pages 16337–16346, 2021.
- [10] Yangsibo Huang, Samyak Gupta, Zhao Song, Kai Li, and Sanjeev Arora. Evaluating gradient inversion attacks and defenses in federated learning. In M. Ranzato, A. Beygelzimer, Y. Dauphin, P.S. Liang, and J. Wortman Vaughan, editors, *Advances in Neural Information Processing Systems*, volume 34, pages 7232–7241. Curran Associates, Inc., 2021.
- [11] Lingjuan Lyu and Chen Chen. A novel attribute reconstruction attack in federated learning. *FTL-IJCAI 2021 : International Workshop on Federated and Transfer Learning for Data Sparsity and Confidentiality*, 2021.
- [12] Matt Fredrikson, Somesh Jha, and Thomas Ristenpart. Model inversion attacks that exploit confidence information and basic countermeasures. In *Proceedings of the 22nd ACM SIGSAC Conference on Computer and Communications Security*, pages 1322–1333, 2015.
- [13] Shiva Prasad Kasiviswanathan, Mark Rudelson, and Adam Smith. The power of linear reconstruction attacks. In *Proceedings of the twenty-fourth annual ACM-SIAM symposium on Discrete algorithms*, pages 1415–1433. SIAM, 2013.
- [14] Matthew Fredrikson, Eric Lantz, Somesh Jha, Simon Lin, David Page, and Thomas Ristenpart. Privacy in pharmacogenetics: An end-to-end case study of personalized warfarin dosing. In *23rd {USENIX} Security Symposium ({USENIX} Security 14)*, pages 17–32, 2014.
- [15] Samuel Yeom, Irene Giacomelli, Matt Fredrikson, and Somesh Jha. Privacy risk in machine learning: Analyzing the connection to overfitting. In *2018 IEEE 31st Computer Security Foundations Symposium (CSF)*, pages 268–282. IEEE, 2018.

- [16] Hongsheng Hu, Zoran Salcic, Lichao Sun, Gillian Dobbie, and Xuyun Zhang. Source inference attacks in federated learning. In *2021 IEEE International Conference on Data Mining (ICDM)*, pages 1102–1107, 2021.
- [17] Yongxin Guo, Tao Lin, and Xiaoying Tang. Fedaug: Reducing the local learning bias improves federated learning on heterogeneous data. *arXiv preprint arXiv:2205.13462*, 2022.
- [18] Ahmed Khaled, Konstantin Mishchenko, and Peter Richtárik. Tighter theory for local sgd on identical and heterogeneous data. In *International Conference on Artificial Intelligence and Statistics*, pages 4519–4529. PMLR, 2020.
- [19] AT&T Laboratories Cambridge. The orl database of faces. <https://www.kaggle.com/datasets/kasikrit/att-database-of-faces>.
- [20] Takayuki Nishio and Ryo Yonetani. Client selection for federated learning with heterogeneous resources in mobile edge. In *2019 IEEE International Conference on Communications (ICC)*, pages 1–7. IEEE, 2019.
- [21] Wenlin Chen, Samuel Horvath, and Peter Richtarik. Optimal client sampling for federated learning. *Workshop in NeurIPS 2020: Privacy Preserving Machine Learning*, 2020.
- [22] Yae Jee Cho, Jianyu Wang, and Gauri Joshi. Towards understanding biased client selection in federated learning. In Gustau Camps-Valls, Francisco J. R. Ruiz, and Isabel Valera, editors, *Proceedings of The 25th International Conference on Artificial Intelligence and Statistics*, volume 151 of *Proceedings of Machine Learning Research*, pages 10351–10375. PMLR, 28–30 Mar 2022.
- [23] Peter Kairouz, H Brendan McMahan, Brendan Avent, Aurélien Bellet, Mehdi Bennis, Arjun Nitin Bhagoji, Kallista Bonawitz, Zachary Charles, Graham Cormode, Rachel Cummings, et al. Advances and open problems in federated learning. *Foundations and Trends® in Machine Learning*, 14(1–2):1–210, 2021.
- [24] Luca Melis, Congzheng Song, Emiliano De Cristofaro, and Vitaly Shmatikov. Exploiting unintended feature leakage in collaborative learning. In *2019 IEEE Symposium on Security and Privacy (SP)*, pages 691–706. IEEE, 2019.
- [25] Milad Nasr, Reza Shokri, and Amir Houmansadr. Comprehensive privacy analysis of deep learning: Passive and active white-box inference attacks against centralized and federated learning. In *2019 IEEE Symposium on Security and Privacy (SP)*, pages 739–753. IEEE, 2019.
- [26] Keith Bonawitz, Vladimir Ivanov, Ben Kreuter, Antonio Marcedone, H. Brendan McMahan, Sarvar Patel, Daniel Ramage, Aaron Segal, and Karn Seth. Practical secure aggregation for privacy-preserving machine learning. In *Proceedings of the 2017 ACM SIGSAC Conference on Computer and Communications Security, CCS '17*, page 1175–1191, New York, NY, USA, 2017. Association for Computing Machinery.
- [27] Swanand Kadhe, Nived Rajaraman, O Ozan Koyluoglu, and Kannan Ramchandran. Fast-secagg: Scalable secure aggregation for privacy-preserving federated learning. *arXiv preprint arXiv:2009.11248*, 2020.
- [28] Do Le Quoc, Franz Gregor, Sergei Arnautov, Roland Kunkel, Pramod Bhatotia, and Christof Fetzer. Securetf: A secure tensorflow framework. In *Proceedings of the 21st International Middleware Conference*, pages 44–59, 2020.
- [29] Peva Blanchard, El Mahdi El Mhamdi, Rachid Guerraoui, and Julien Stainer. Machine learning with adversaries: Byzantine tolerant gradient descent. *Advances in neural information processing systems*, 30, 2017.
- [30] Dong Yin, Yudong Chen, Ramchandran Kannan, and Peter Bartlett. Byzantine-robust distributed learning: Towards optimal statistical rates. In *International Conference on Machine Learning*, pages 5650–5659. PMLR, 2018.
- [31] El Mahdi El Mhamdi. *Robust Distributed Learning*. PhD thesis, EPFL, February 2020.

- [32] Florian Tramèr, Reza Shokri, Ayrton San Joaquin, Hoang Le, Matthew Jagielski, Sanghyun Hong, and Nicholas Carlini. Truth serum: Poisoning machine learning models to reveal their secrets. In *ACM CCS*, 2022.
- [33] Mohamed Sabt, Mohammed Achemlal, and Abdelmadjid Bouabdallah. Trusted execution environment: What it is, and what it is not. In *2015 IEEE Trustcom/BigDataSE/ISPA*, volume 1, pages 57–64, 2015.
- [34] Jatinder Singh, Jennifer Cobbe, Do Le Quoc, and Zahra Tarkhani. Enclaves in the clouds: Legal considerations and broader implications. *Commun. ACM*, 64(5):42–51, apr 2021.
- [35] Leonid I Rudin, Stanley Osher, and Emad Fatemi. Nonlinear total variation based noise removal algorithms. *Physica D: nonlinear phenomena*, 60(1-4):259–268, 1992.
- [36] Xiaoxiao Li, Meirui Jiang, Xiaofei Zhang, Michael Kamp, and Qi Dou. Fedbn: Federated learning on non-iid features via local batch normalization. In *9th International Conference on Learning Representations, ICLR 2021, Virtual Event, Austria, May 3-7, 2021*, 2021.
- [37] Martin Abadi, Andy Chu, Ian Goodfellow, H. Brendan McMahan, Ilya Mironov, Kunal Talwar, and Li Zhang. Deep learning with differential privacy. In *Proceedings of the 2016 ACM SIGSAC Conference on Computer and Communications Security*. ACM, oct 2016.
- [38] Borja Balle, Gilles Barthe, and Marco Gaboardi. Privacy amplification by subsampling: Tight analyses via couplings and divergences. In *Advances in Neural Information Processing Systems*, pages 6277–6287, 2018.
- [39] Yu-Xiang Wang, Borja Balle, and Shiva Prasad Kasiviswanathan. Subsampled rényi differential privacy and analytical moments accountant. In *The 22nd International Conference on Artificial Intelligence and Statistics*, pages 1226–1235. PMLR, 2019.
- [40] Hongyi Zhang, Moustapha Cissé, Yann N. Dauphin, and David Lopez-Paz. mixup: Beyond empirical risk minimization. In *6th International Conference on Learning Representations, ICLR 2018, Vancouver, BC, Canada, April 30 - May 3, 2018, Conference Track Proceedings*, 2018.
- [41] Tehrim Yoon, Sumin Shin, Sung Ju Hwang, and Eunho Yang. Fedmix: Approximation of mixup under mean augmented federated learning. In *9th International Conference on Learning Representations, ICLR 2021, Virtual Event, Austria, May 3-7, 2021*, 2021.
- [42] Jie Zhang, Chen Chen, Bo Li, Lingjuan Lyu, Shuang Wu, Shouhong Ding, Chunhua Shen, and Chao Wu. Dense: Data-free one-shot federated learning. In *Advances in Neural Information Processing Systems*.
- [43] Sidak Pal Singh and Martin Jaggi. Model fusion via optimal transport. In H. Larochelle, M. Ranzato, R. Hadsell, M.F. Balcan, and H. Lin, editors, *Advances in Neural Information Processing Systems*, volume 33, pages 22045–22055. Curran Associates, Inc., 2020.
- [44] Dheeru Dua and Casey Graff. UCI machine learning repository, 2017.
- [45] Sebastian Caldas, Sai Meher Karthik Duddu, Peter Wu, Tian Li, Jakub Konečný, H. Brendan McMahan, Virginia Smith, and Ameet Talwalkar. Leaf: A benchmark for federated settings. In *Workshop on Federated Learning for Data Privacy and Confidentiality (2019)*, 2019.
- [46] Bargav Jayaraman and David Evans. Evaluating differentially private machine learning in practice. In *28th {USENIX} Security Symposium ({USENIX} Security 19)*, pages 1895–1912, 2019.
- [47] Florian Tramèr, Fan Zhang, Ari Juels, Michael K Reiter, and Thomas Ristenpart. Stealing machine learning models via prediction apis. In *25th {USENIX} Security Symposium ({USENIX} Security 16)*, pages 601–618, 2016.
- [48] Zhibo Wang, Mengkai Song, Zhifei Zhang, Yang Song, Qian Wang, and Hairong Qi. Beyond inferring class representatives: User-level privacy leakage from federated learning. In *2019 IEEE Conference on Computer Communications (INFOCOM)*, page 2512–2520. IEEE Press, 2019.

- [49] Nisarg Raval, Ashwin Machanavajjhala, and Jerry Pan. Olympus: Sensor privacy through utility aware obfuscation. *Proc. Priv. Enhancing Technol.*, 2019(1):5–25, 2019.
- [50] Mengkai Song, Zhibo Wang, Zhifei Zhang, Yang Song, Qian Wang, Ju Ren, and Hairong Qi. Analyzing user-level privacy attack against federated learning. *IEEE Journal on Selected Areas in Communications*, 38(10):2430–2444, 2020.
- [51] Hengrui Jia, Hongyu Chen, Jonas Guan, Ali Shahin Shamsabadi, and Nicolas Papernot. A zest of LIME: Towards architecture-independent model distances. In *International Conference on Learning Representations*, 2022.
- [52] Marco Tulio Ribeiro, Sameer Singh, and Carlos Guestrin. "why should i trust you?": Explaining the predictions of any classifier. In *Proceedings of the 22nd ACM SIGKDD International Conference on Knowledge Discovery and Data Mining*, KDD '16, page 1135–1144, New York, NY, USA, 2016. Association for Computing Machinery.
- [53] Zhou Wang, A.C. Bovik, H.R. Sheikh, and E.P. Simoncelli. Image quality assessment: from error visibility to structural similarity. *IEEE Transactions on Image Processing*, 13(4):600–612, 2004.
- [54] Cynthia Dwork, Frank McSherry, Kobbi Nissim, and Adam Smith. Calibrating noise to sensitivity in private data analysis. In Shai Halevi and Tal Rabin, editors, *Theory of Cryptography*, pages 265–284, Berlin, Heidelberg, 2006. Springer Berlin Heidelberg.
- [55] Yurii Nesterov. *Introductory lectures on convex optimization: A basic course*, volume 87. Springer Science & Business Media, 2003.
- [56] Alekh Agarwal, Sahand Negahban, and Martin J Wainwright. Stochastic optimization and sparse statistical recovery: Optimal algorithms for high dimensions. *Advances in Neural Information Processing Systems*, 25, 2012.
- [57] Chi Jin, Rong Ge, Praneeth Netrapalli, Sham M. Kakade, and Michael I. Jordan. How to escape saddle points efficiently. In Doina Precup and Yee Whye Teh, editors, *Proceedings of the 34th International Conference on Machine Learning*, volume 70 of *Proceedings of Machine Learning Research*, pages 1724–1732. PMLR, 06–11 Aug 2017.
- [58] Stefan Vlaski and Ali H. Sayed. Distributed learning in non-convex environments—part i: Agreement at a linear rate. *IEEE Transactions on Signal Processing*, 69:1242–1256, 2021.
- [59] Xiaoyu Li and Francesco Orabona. A high probability analysis of adaptive sgd with momentum. In *Workshop on Beyond First Order Methods in ML Systems at ICML'20*, 2020.
- [60] Dongruo Zhou, Jinghui Chen, Yuan Cao, Yiqi Tang, Ziyang Yang, and Quanquan Gu. On the convergence of adaptive gradient methods for nonconvex optimization. In *OPT2020: 12th Annual Workshop on Optimization for Machine Learning*, 2020.
- [61] J. Shao. *Mathematical Statistics*. Springer Texts in Statistics. Springer, 2003.
- [62] Philippe Rigollet. Lecture notes: High-dimensional statistics. [https://ocw.mit.edu/courses/mathematics/18-s997-high-dimensional-statistics-spring-2015/lecture-notes/MIT18\\_S997S15\\_Chapter2.pdf](https://ocw.mit.edu/courses/mathematics/18-s997-high-dimensional-statistics-spring-2015/lecture-notes/MIT18_S997S15_Chapter2.pdf).
- [63] A.N. Kolmogorov, S.V. Fomin, and S.V. Fomin. *Elements of the Theory of Functions and Functional Analysis*. Number v. 1 in Dover books on mathematics. Dover, 1999.
- [64] Rodrigo Acuna-Agost et al. Price elasticity estimation for deep learning-based choice models: An application to air itinerary choices. *Journal of Revenue and Pricing Management*, 20(3):213–226, 2021.
- [65] Xiang Li, Kaixuan Huang, Wenhao Yang, Shusen Wang, and Zhihua Zhang. On the convergence of fedavg on non-iid data. In *8th International Conference on Learning Representations, ICLR 2020, Addis Ababa, Ethiopia, April 26-30, 2020*, 2020.

- [66] Sergey Ioffe and Christian Szegedy. Batch normalization: Accelerating deep network training by reducing internal covariate shift. In *Proceedings of the 32nd International Conference on International Conference on Machine Learning - Volume 37*, ICML'15, page 448–456. JMLR.org, 2015.
- [67] Olivia Choudhury, Aris Gkoulalas-Divanis, Theodoros Salonidis, Issa Sylla, Yoonyoung Park, Grace Hsu, and Amar Das. Differential privacy-enabled federated learning for sensitive health data. *Workshop on Machine learning for Health in NeurIPS*, 2019.
- [68] Ashkan Yousefpour, Igor Shilov, Alexandre Sablayrolles, Davide Testuggine, Karthik Prasad, Mani Malek, John Nguyen, Sayan Ghosh, Akash Bharadwaj, Jessica Zhao, Graham Cormode, and Ilya Mironov. Opacus: User-friendly differential privacy library in pytorch, 2021.
- [69] Tianyu Pang, Kun Xu, and Jun Zhu. Mixup inference: Better exploiting mixup to defend adversarial attacks. In *8th International Conference on Learning Representations, ICLR 2020, Addis Ababa, Ethiopia, April 26-30, 2020*, 2020.

## A Local update rule of every client in FedAvg [1]

---

**Algorithm 3** Client  $c$ 's local update rule in FedAvg [1]

---

Local\_Update $^c(\theta, \mathcal{D}_c)$

$\theta$ : server model,  $\mathcal{D}_c$ : local dataset,  $B$ : batch size,  $E$ : the number of local epochs,  $\eta$ : learning rate.

- 1:  $\theta_c \leftarrow \theta, \mathcal{B} \leftarrow$  (split  $\mathcal{D}_c$  into batches of size  $B$ )
  - 2: **for** each local epoch  $e$  from 1 to  $E$  **do**
  - 3:   **for** batch  $b \in \mathcal{B}$  **do**
  - 4:      $\theta_c \leftarrow \theta_c - \eta \times \mathbf{g}(\theta_c, b)$ , where  $\mathbf{g}(\theta_c, b) = \frac{1}{B} \sum_{x \in b} \nabla l(\theta_c, x)$
  - 5: **Return**  $\theta_c$
- 

## B Proofs

### B.1 Theoretical guarantees on model-based AIA

Here, we give the bound for the accuracy of model-based AIA shown in Problem (3), considering a least squares regression model with binary sensitive attributes.

**Proposition 4.** Let  $\mathbf{s}_c$  be the vector including all the unknown sensitive binary attributes  $\{s_c(i), \forall i \in \{1, \dots, S_c\}\}$  of client  $c$ . Let  $E_c$  be the mean square error of a given ML least squares regression model  $\theta$  on the local dataset of client  $c$  and  $\theta[s]$  be the model parameter corresponding to the sensitive attribute. The accuracy to recover  $\mathbf{s}_c$  is larger than or equal to  $1 - \frac{4E_c}{\theta[s]^2}$ .

*Proof.* Let  $\mathbf{x}_c \in \mathbb{R}^{S_c \times d}$  be the design matrix with rank  $d$  and  $\mathbf{y}_c \in \mathbb{R}^{S_c}$  be the labels in the local dataset  $\mathcal{D}_c$  of the client  $c$ . Let  $\theta[:p] \in \mathbb{R}^{d-1}$  be the parameters corresponding to the public attributes. The adversary has access to partial data instances in  $\mathcal{D}_c$  which consists of the public attributes  $\mathbf{P} \in \mathbb{R}^{S_c \times (d-1)}$  and the corresponding labels  $\mathbf{y}_c \in \mathbb{R}^{S_c}$ .

The goal for the adversary is to decode the values of the binary sensitive attribute  $\mathbf{s}_c \in \{0, 1\}^{S_c}$  given  $(\mathbf{P}, \mathbf{y}_c)$  by solving Problem 3, which is

$$\tilde{\mathbf{s}}_c = \arg \min_{\mathbf{s}_c \in \mathbb{R}^{S_c}} \|\mathbf{P}\theta[:p] + \mathbf{s}_c\theta[s] - \mathbf{y}_c\|_2^2 = \frac{\mathbf{y}_c - \mathbf{P}\theta[:p]}{\theta[s]}.$$

Then, the adversary can reconstruct the sensitive values in  $\hat{\mathbf{s}}_c = [\hat{s}(1), \hat{s}(2), \dots, \hat{s}(S_c)]$ , that

$$\hat{s}(i) = \begin{cases} 0 & \text{if } \tilde{\mathbf{s}}_c(i) < \frac{1}{2}, \\ 1 & \text{otherwise} \end{cases}, \quad \forall i \in \{1, \dots, S_c\}. \quad (9)$$

Now we start to evaluate the difference between the recovered  $\hat{\mathbf{s}}_c$  and the true labels  $\mathbf{s}_c$ . Let  $\mathbf{e}$  be the vector of residuals for the public data, i.e.,  $\mathbf{e} = \mathbf{y}_c - (\mathbf{P}\theta[:p] + \mathbf{s}_c\theta[s])$ . We have then

$$\mathbf{s}_c = \frac{\mathbf{y}_c - \mathbf{P}\theta[:p] - \mathbf{e}}{\theta[s]} = \tilde{\mathbf{s}}_c - \frac{\mathbf{e}}{\theta[s]}. \quad (10)$$

According to Eqs. 9 and 10, we know that the prediction entry in  $\hat{\mathbf{s}}_c$  differs from  $\mathbf{s}_c$  only when the corresponding entry in  $\frac{\mathbf{e}}{\theta[s]}$  has absolute value above  $1/2$ . Let  $E_c$  be the mean square error of the accessible data instance, i.e.,  $E_c = \frac{\|\mathbf{e}\|_2^2}{S_c}$ . We have  $\|\mathbf{e}\|_2^2 = E_c \times S_c$  and  $\|\frac{\mathbf{e}}{\theta[s]}\|_2^2 = \frac{E_c \times S_c}{\theta[s]^2}$ . This implies that  $\frac{\mathbf{e}}{\theta[s]}$  cannot have more than  $\lfloor \frac{4E_c \times S_c}{\theta[s]^2} \rfloor$  entries with absolute value above  $1/2$ . Therefore, the success of the attack is larger than or equal to  $1 - \frac{4E_c}{\theta[s]^2}$ .  $\square$

From Proposition 4, we can see that the accuracy of the attack depends on the importance of the sensitive attribute in model  $\theta$  and how well the model fits the data. If the model fits perfectly the known data, the attack can achieve 100% of the accuracy on these data.

## B.2 Proof of Proposition 1

We start with a lemma used in Proposition 1.

**Lemma 1.** *Let  $\mathbf{A}$  be a symmetric positive definite matrix.  $\mathbf{I} - (\mathbf{I} - \mathbf{A})^n$  is invertible for  $n \geq 0$ .*

*Proof.* Since  $\mathbf{A}$  is positive definite and symmetric, it can be decomposed to  $\mathbf{U}\Lambda\mathbf{U}^T$ , where  $\mathbf{U}\mathbf{U}^T = \mathbf{I}$  and  $\Lambda$  is a diagonal matrix whose entries are the positive eigenvalues of  $\mathbf{A}$ . Thus we have

$$\begin{aligned}\mathbf{I} - (\mathbf{I} - \mathbf{A})^n &= \mathbf{U}\mathbf{U}^T - (\mathbf{U}\mathbf{U}^T - \mathbf{U}\Lambda\mathbf{U}^T)^n = \mathbf{U}\mathbf{U}^T - \mathbf{U}(\mathbf{I} - \Lambda)^n\mathbf{U}^T \\ &= \mathbf{U}(\mathbf{I} - (\mathbf{I} - \Lambda)^n)\mathbf{U}^T.\end{aligned}$$

Since  $\Lambda$  is with only positive values on diagonal, eigenvalues of  $\mathbf{I} - (\mathbf{I} - \mathbf{A})^n$  are non-zeros. So  $\mathbf{I} - (\mathbf{I} - \mathbf{A})^n$  is invertible and its inverse is  $\mathbf{U}(\mathbf{I} - (\mathbf{I} - \Lambda)^n)^{-1}\mathbf{U}^T$ .  $\square$

The main proof of Proposition 1 is presented below.

*Proof.* Let  $\mathbf{x}_c \in \mathbb{R}^{m \times d}$  be the design matrix at client  $c$  and  $\mathbf{y}_c \in \mathbb{R}^m$  be the labels in the local dataset  $\mathcal{D}_c$  with size  $m = |\mathcal{D}_c|$ .

$$\mathcal{L}_c(\theta) = \frac{\|\mathbf{x}_c\theta - \mathbf{y}_c\|^2}{m} \quad (11)$$

Let  $\mathbf{H} = \mathbf{x}_c^T \mathbf{x}_c$ . We know that  $\theta_c^* = (\mathbf{x}_c^T \mathbf{x}_c)^{-1} \mathbf{x}_c^T \mathbf{y}_c$ . When the batch size is set to  $m$  in FedAvg:

$$\mathbf{g}(\theta) = \frac{2}{m} (\mathbf{H}\theta - \mathbf{H}\theta_c^*). \quad (12)$$

At round  $t$ , if selected, client  $c$  receives the server model and executes Algorithm 3. Let  $\theta_c^t(e)$  be the model after the  $e$ -th local epoch's update. Replacing (12) in line 4 of Algorithm 3, we have

$$\begin{aligned}\theta_c^t(E) &= \theta_c^t(E-1) - \frac{2\eta}{m} (\mathbf{H}\theta_c^t(E-1) - \mathbf{H}\theta_c^*) \\ &= (\mathbf{I} - \frac{2\eta}{m} \mathbf{H})\theta_c^t(E-1) + \frac{2\eta}{m} \mathbf{H}\theta_c^* \\ &= (\mathbf{I} - \frac{2\eta}{m} \mathbf{H})^E \theta_c^t(0) + \left[ \mathbf{I} - (\mathbf{I} - \frac{2\eta}{m} \mathbf{H})^E \right] \theta_c^*.\end{aligned} \quad (13)$$

Let  $\mathbf{W} = [\mathbf{I} - (\mathbf{I} - \frac{2\eta}{m} \mathbf{H})^E]$  and  $\mathbf{v} = \mathbf{W}\theta_c^*$ . We have

$$\theta_c^t(0) - \theta_c^t(E) = \left[ \mathbf{I} - \left( \mathbf{I} - \frac{2\eta}{m} \mathbf{H} \right)^E \right] \theta_c^t(0) - \left[ \mathbf{I} - \left( \mathbf{I} - \frac{2\eta}{m} \mathbf{H} \right)^E \right] \theta_c^* \quad (14)$$

$$= \mathbf{W}\theta_c^t(0) - \mathbf{v}. \quad (15)$$

Note that  $\theta_c^t(0)$  is the server model and  $\theta_c^t(E)$  is model returned from client  $c$  to the server in Algorithm 3. The adversary has access to both of them as it can eavesdrop messages exchanged between the server and the client. Since  $\mathbf{W} \in \mathbb{R}^{d \times d}$  and  $\mathbf{v} \in \mathbb{R}^d$ , once the adversary gets  $d+1$  exchanged messages, it can reconstruct the exact matrix  $\mathbf{W}$  and the vector  $\mathbf{v}$  by solving  $d$  systems (one for each row of  $\mathbf{W}$  and the corresponding element of  $\mathbf{v}$  in (15)), each with  $d+1$  linear equations (one for each communication round). Solving a system of  $d+1$  linear equations requires  $O(d^3)$  operations, thus solving  $d$  systems requires  $O(d^4)$  operations. Since  $\mathbf{H}$  is positive definite and symmetric,  $\mathbf{W}$  is invertible (Lemma 1). Then, we can compute  $\theta_c^* = \mathbf{W}^{-1}\mathbf{v}$ . Note that in this reconstruction process, the adversary does not require the knowledge of the FedAvg hyperparameters, such as the learning rate and the number of local steps.  $\square$

## B.3 Proof of Proposition 2

*Proof.* To prove the lower bound for the communications, we construct a specific "hard" scenario. This scenario is inspired by the lower bound for the convergence of gradient methods minimizing smooth convex functions [55, Sect. 2.1.2].

Let  $\mathbf{c}$  be the client having the local dataset  $(\mathbf{x}_c, \mathbf{y}_c)$  such that  $\mathbf{H}_c = \mathbf{x}_c^T \mathbf{x}_c$  is a tridiagonal matrix with  $\mathbf{H}_c[i, i+1] = \mathbf{H}_c[i+1, i] = -1/2$  and  $\mathbf{H}_c[i, i] = 1, \forall i \in \{1, 2, \dots, d\}$ , and  $\mathbf{x}_c^T \mathbf{y}_c = [1/2, 0, 0, \dots, 0]^T$ .<sup>9</sup> By substituting  $\mathbf{H}_c$  and  $\mathbf{x}_c^T \mathbf{y}_c$  into (11), we have

$$\begin{aligned} \mathcal{L}_c(\theta) &= \frac{1}{m} (\theta^T \mathbf{H}_c \theta - 2(\mathbf{x}_c^T \mathbf{y}_c)^T \theta - \mathbf{y}_c^T \mathbf{y}_c) \\ &= \frac{1}{m} \left( \sum_{i=1}^d \theta_{[i]}^2 - \sum_{i=1}^{d-1} \theta_{[i]} \theta_{[i+1]} - \theta_{[1]} - C \right), \end{aligned} \quad (16)$$

where  $C = \mathbf{y}_c^T \mathbf{y}_c$  is a constant and  $\theta_c^* = \arg \min \mathcal{L}_c(\theta) = (\mathbf{H}_c)^{-1} \mathbf{x}_c^T \mathbf{y}_c = [1 - \frac{1}{d+1}, 1 - \frac{2}{d+1}, \dots, 1 - \frac{d}{d+1}]^T$  [55]. According to (16), we know that if  $\theta_{[i]} = \theta_{[i+1]} = \dots = \theta_{[d]} = 0$ , then  $\nabla \mathcal{L}_c(\theta)_{[i+1]} = \dots = \nabla \mathcal{L}_c(\theta)_{[d]} = 0$ .

At the same time, for any other client  $\forall \bar{c} \in \mathcal{C} \setminus \{\mathbf{c}\}$ , we assume their local optimum are zeros where their local dataset  $\mathbf{X}_{\bar{c}} = \mathbf{I}$  and  $\mathbf{y}_{\bar{c}} = \mathbf{0}$ . In this setting, according to (13), we know that if the  $i^{\text{th}}$  element of the global model is zero, i.e.,  $\theta(t)_{[i]} = 0$ , then  $\theta_{\bar{c}}^t(E)_{[i]} = 0$ .

Let  $n = |\mathcal{C}|$  be the number of clients and assume that every client has  $m$  local data samples. Then the global empirical risk and its gradients have the following expressions:

$$\mathcal{L}(\theta) = \frac{1}{nm} \left( \sum_{i=1}^d n \times \theta_{[i]}^2 - \sum_{i=1}^{d-1} \theta_{[i]} \theta_{[i+1]} - \theta_{[1]} - C' \right), \quad (17)$$

$$\nabla \mathcal{L}(\theta)_{[1]} = \frac{1}{nm} (2n \times \theta_{[1]} - \theta_{[2]} - 1), \quad (18)$$

$$\nabla \mathcal{L}(\theta)_{[i]} = \frac{1}{nm} (2n \times \theta_{[i]} - \theta_{[i-1]} - \theta_{[i+1]}), \forall i \in \{2, \dots, d-1\}, \quad (19)$$

$$\nabla \mathcal{L}(\theta)_{[d]} = \frac{1}{nm} (2n \times \theta_{[d]} - \theta_{[d-1]}), \quad (20)$$

where  $C'$  is a constant. According to (18), (19) and (20), the global optimum  $\theta^*$  satisfies:

$$\theta_{[1]}^* = (1 + \theta_{[2]}^*)/2n, \quad (21)$$

$$\theta_{[i]}^* = 2n\theta_{[i+1]}^* - \theta_{[i+2]}^*, \forall i \in \{1, \dots, d-2\}, \quad (22)$$

$$\theta_{[d-1]}^* = 2n\theta_{[d]}^*. \quad (23)$$

Equations 22 and 23 show that  $\theta_{[i]}^*$  is proportional to  $\theta_{[d]}^*$  for every  $i \in \{1, \dots, d-1\}$ , i.e.,  $\theta_{[i]}^* = k_i \times \theta_{[d]}^*$  where  $k_i > 0$ . Since  $\theta_{[1]}^* = k_1 \times \theta_{[d]}^*$  and  $\theta_{[2]}^* = k_2 \times \theta_{[d]}^*$  where  $k_1 > 0$  and  $k_2 > 0$ , by substituting  $\theta_{[1]}^*$  and  $\theta_{[2]}^*$  into (21), we can see that  $\theta_{[d]}^* \neq 0$ . Therefore, we can prove then that every element of the global optimum is non-zero, i.e.,  $\theta_{[i]}^* \neq 0, \forall i \in \{1, \dots, d\}$ .

Now, suppose that we run the FedAvg with one local step under the above scenario, with initial global model  $\theta(0) = \mathbf{0}$ , i.e.,  $\theta_c^0(0) = \mathbf{0}, \forall c \in \mathcal{C}$ . According to the previous analysis, we know that  $\forall t \in \{0, 1, \dots, d-1\}$ :

$$\theta_c^t(E)_{[t+1]} = \theta_c^t(E)_{[t+2]} = \dots = \theta_c^t(E)_{[d]} = 0, \quad (24)$$

and

$$\theta(t)_{[t+1]} = \theta(t)_{[t+2]} = \dots = \theta(t)_{[d]} = 0. \quad (25)$$

Therefore, to reach the non-zeros global optimum, the client  $\mathbf{c}$  needs to communicate with the server (be selected by the server) at least  $d$  times.

Moreover, to recover the local optimum of client  $\mathbf{c}$ , the adversary must listen on the communication channel for at least  $d$  times. In fact, suppose that the client  $\mathbf{c}$  holds another local data set which gives  $\mathbf{H}'_c$  equals to  $\mathbf{H}_c$  but for the last row and the last column that are zeros. Under this case, the adversary will have the same observation under  $\mathbf{H}_c$  and under  $\mathbf{H}'_c$  till round  $d-1$ .  $\square$

<sup>9</sup>One example for the local data  $(\mathbf{x}_c, \mathbf{y}_c)$  satisfying the condition:  $\mathbf{x}_c \in \mathbb{R}^{d \times d}$  with  $\mathbf{x}_c[1, 1] = 1; \mathbf{x}_c[i+1, i+1] = \sqrt{1 - \frac{1}{4\mathbf{x}_c[i, i]^2}}$  and  $\mathbf{x}_c[i+1, i] = \frac{-1}{2\mathbf{x}_c[i, i]}, \forall i \in \{1, \dots, d-1\}; \mathbf{x}_c[i, i+1] = \mathbf{x}_c[i, j] = 0, \forall |i-j| \geq 1$ .  $\mathbf{y}_c \in \mathbb{R}^d$  with  $\mathbf{y}_c[1] = \frac{1}{2}$  and  $\mathbf{y}_c[i+1] = \frac{-\mathbf{x}_c[i+1, i] \mathbf{y}_c[i]}{\mathbf{x}_c[i+1, i+1]}, \forall i \in \{1, \dots, d-1\}$ .

#### B.4 Proof of stochastic case

**Proposition 3.** Consider training a least squares regression through FedAvg with  $\mathcal{T}_c = \{t_1, t_2, \dots, t_{n_c}\}$  the  $n_c$  rounds at which the adversary inspects the messages. Assume that

1. the client’s design matrix  $\mathbf{x}_c \in \mathbb{R}^{m \times d}$  has rank  $d$  equal to the number of features;
2. the distribution of the stochastic (mini-batch) gradient for each dimension is sub-Gaussian with variance proxy  $\sigma^2$ , i.e.,

$$\mathbb{E}[\exp(\mathbf{e}(\theta)[i]/\sigma^2)] \leq \exp(1), \forall \theta, \forall i \in \{1, 2, \dots, d\},$$

where  $\mathbf{e}(\theta) = \mathbf{g}(\theta) - \nabla \mathcal{L}_c(\theta)$ ;<sup>10</sup>

3. the input model vectors at an observed round are independent of the previous stochastic gradients computed by the attacked client;
4. there exists  $\underline{\lambda} > 0$  such that  $\forall n_c \in \mathbb{N}$ , we can always select  $n_c$  observation rounds so that

$$\lambda_{\min} \left( \frac{\Theta_{in}^T \Theta_{in}}{n_c} \right) \geq \underline{\lambda}, \text{ where } \Theta_{in} = \begin{bmatrix} \theta^{t_1}(0)^T & 1 \\ \vdots & \\ \theta^{t_{n_c}}(0)^T & 1 \end{bmatrix}, \text{ and } \lambda_{\min}(\mathbf{A}) \text{ denotes the smallest eigenvalue of the matrix } \mathbf{A}.$$

The error of the reconstructed model  $\hat{\theta}_c^*$ , i.e.,  $\|\hat{\theta}_c^* - \theta_c^*\|_2$ , is upper bounded w.h.p. when  $\eta \leq \frac{m}{2\lambda_{\max}(\mathbf{x}_c^T \mathbf{x}_c)}$ . More precisely,

$$\|\theta_c^* - \hat{\theta}_c^*\|_2 \leq \frac{2\eta\sigma d}{\lambda_{\min}(\mathbf{W})} (\|\theta_c^*\|_2 + 1) \sqrt{E \left[ \frac{m}{b} \right] \frac{d+1+\ln \frac{2}{\delta}}{n_c \cdot \underline{\lambda}}}, \text{ w.p. } \geq 1 - \delta. \quad (26)$$

Before presenting the proof, we discuss the assumptions. The first assumption can be relaxed at the cost of replacing in the proof the inverse  $\mathbf{H}^{-1}$  of the matrix  $\mathbf{H} = \mathbf{x}_c^T \mathbf{x}_c$  by its pseudo-inverse  $\mathbf{H}^\dagger$ . The second assumption is common in the analysis of stochastic gradient methods [56–60]. The third assumption is technically not satisfied in our scenario as the stochastic gradients computed by the attacked client  $i$  before an observed round  $t_n$  have contributed to determine the models sent back by client  $i$  at rounds  $t < t_n$  and then the global model  $\theta^{t_n}(0)$  sent by the server to client  $i$ . Nevertheless, we observe that  $\theta^{t'}(0)$  is almost independent on client- $i$ ’s stochastic gradients if the set of clients is very large. Moreover, the assumption is verified if we assume a more powerful adversary who can act as a man in the middle and modify the model sent to the client. Finally, the fourth assumption corresponds to the “well-behaved data assumption” for a generic linear regression problem, which is required to be able to prove the consistency of the estimators, i.e., that they converge with probability 1 to the correct value as the number of samples diverges. If the input feature matrix is  $\mathbf{X}$ , this assumption can be expressed as  $\frac{\mathbf{X}^T \mathbf{X}}{n} \xrightarrow{n \rightarrow +\infty} \mathbf{Q}$ , where  $\mathbf{Q}$  is a positive definite matrix, and this implies the existence of a positive lower bound for  $\lambda_{\min} \left( \frac{\mathbf{X}^T \mathbf{X}}{n} \right)$  (see for example [61, Lem. 3.3]).

*Proof.* Let  $\mathbf{H} = \mathbf{x}_c^T \mathbf{x}_c$  which is positive definite. Let  $\mathbf{y}_c \in \mathbb{R}^m$  be the labels in the local dataset  $\mathcal{D}_c$  with size  $m = |\mathcal{D}_c|$ .

$$\mathcal{L}_c(\theta) = \frac{\|\mathbf{x}_c \theta - \mathbf{y}_c\|_2^2}{m} \quad (27)$$

We know that  $\theta_c^* = (\mathbf{x}_c^T \mathbf{x}_c)^{-1} \mathbf{x}_c^T \mathbf{y}_c$ . When computing the stochastic gradient, we have:

$$\mathbf{g}(\theta) = \nabla \mathcal{L}_c(\theta) + \mathbf{e}(\theta) = \frac{2}{m} (\mathbf{H}\theta - \mathbf{H}\theta_c^*) + \mathbf{e}(\theta). \quad (28)$$

At round  $t$ , if selected, client  $c$  receives the server model and executes Algorithm 3. Let  $\theta_c^t(k)$  be the model after the  $k$ -th local update. To simplify the notation, in the following, we replace  $\mathbf{e}(\theta)$  by  $\mathbf{e}_k$ .

<sup>10</sup>Note that, by Jensen’s inequality, this condition implies a bounded variance on the stochastic gradients for each dimension.

Remind that in each epoch, there are  $\lceil \frac{m}{b} \rceil$  local steps where  $b$  is the batch size. Replacing (28) in line 4 of Algorithm 3, we have

$$\begin{aligned} \theta_c^t(E) &= \left( \mathbf{I} - \frac{2\eta}{m} \mathbf{H} \right)^{E \lceil \frac{m}{b} \rceil} \theta_c^t(0) + \left[ \mathbf{I} - \left( \mathbf{I} - \frac{2\eta}{m} \mathbf{H} \right)^{E \lceil \frac{m}{b} \rceil} \right] \theta_c^* \\ &\quad - \sum_{k=1}^{E \lceil \frac{m}{b} \rceil} \left( \mathbf{I} - \frac{2\eta}{m} \mathbf{H} \right)^{k-1} \eta \mathbf{e}_{E \lceil \frac{m}{b} \rceil - k + 1}. \end{aligned}$$

We denote by  $\gamma = -\eta \sum_{k=1}^{E \lceil \frac{m}{b} \rceil} \left( \mathbf{I} - \frac{2\eta}{m} \mathbf{H} \right)^{k-1} \mathbf{e}$ . Let  $\mathbf{x}[i]$  be the  $i^{\text{th}}$  element of vector  $\mathbf{x}$  and  $\mathbf{X}[i : ]$  be the  $i^{\text{th}}$  row of the matrix  $\mathbf{X}$ . Since every element in  $\mathbf{e}$  is sub-Gaussian and the weighted sum of independent sub-Gaussian variables is still sub-Gaussian,  $\gamma[i]$  is sub-Gaussian with  $\mathbb{E}[\gamma[i]] = 0$  and  $\text{Var}[\gamma[i]] \leq \eta^2 \sigma^2 \sum_{k=1}^{E \lceil \frac{m}{b} \rceil} \left\| \left( \mathbf{I} - \frac{2\eta}{m} \mathbf{H} \right)^{k-1} [i : ] \right\|_2^2$ .

Let  $\mathbf{W} = \left[ \mathbf{I} - \left( \mathbf{I} - \frac{2\eta}{m} \mathbf{H} \right)^{E \lceil \frac{m}{b} \rceil} \right]$  and  $\mathbf{v} = \mathbf{W} \theta_c^*$ .

Then we have:

$$(\theta^t(0) - \theta^t(E)) [i] = \mathbf{W}[i : ] \theta^t(0) - \mathbf{v}[i] + \gamma[i], \quad (29)$$

Here, we will bound  $\text{Var}[\gamma[i]]$ .

$$\begin{aligned} \text{Var}[\gamma[i]] &\leq \eta^2 \sigma^2 \sum_{k=1}^{E \lceil \frac{m}{b} \rceil} \left\| \left( \mathbf{I} - \frac{2\eta}{m} \mathbf{H} \right)^{k-1} \right\|_2^2 \\ &= \eta^2 \sigma^2 \sum_{k=1}^{E \lceil \frac{m}{b} \rceil} \rho_{\max}^2 \left( \left( \mathbf{I} - \frac{2\eta}{m} \mathbf{H} \right)^{k-1} \right), \end{aligned}$$

where  $\rho_{\max}(\mathbf{A})$  is the spectral radius of matrix  $\mathbf{A}$ .

Let  $\Lambda$  be a diagonal matrix whose entries are the positive eigenvalues of  $\mathbf{H}$  and  $\lambda_{\max}(\mathbf{H})$  be the largest eigenvalue of  $\mathbf{H}$ , i.e.,  $\lambda_{\max}(\mathbf{H}) = \|\Lambda\|_1$ . When  $\eta \leq \frac{m}{2\lambda_{\max}(\mathbf{H})}$ , the diagonal values in  $\frac{2\eta}{m} \Lambda$  are positive and smaller than or equal to 1. Moreover, the matrix  $\left( \mathbf{I} - \frac{2\eta}{m} \mathbf{H} \right)^{k-1}$  is positive semi-definite and we have  $\rho_{\max} \left[ \left( \mathbf{I} - \frac{2\eta}{m} \mathbf{H} \right)^{k-1} \right] \leq 1$ . Thus, we have

$$\text{Var}[\gamma[i]] \leq \eta^2 \sigma^2 \times E \left\lceil \frac{m}{b} \right\rceil. \quad (30)$$

Since  $\mathbf{v} = \mathbf{W} \theta_c^*$ , if we have  $\mathbf{W}$  and  $\mathbf{v}$ , we can then compute  $\theta_c^* = \mathbf{W}^{-1} \mathbf{v}$ . So for the first step to decode  $\mathbf{W}$  and  $\mathbf{v}$ , we can use the ordinary least squares (OLS) estimator, solving  $d$  multivariate linear regression problems (one for each row of  $\mathbf{W}$  and  $\mathbf{v}$ ), which can be jointly expressed in the following form:

$$\begin{pmatrix} \hat{\mathbf{W}}^T \\ \hat{\mathbf{v}}^T \end{pmatrix} = \underset{\mathbf{W}, \mathbf{v}}{\text{argmin}} \left\| \Theta_{\text{out}} - \Theta_{\text{in}} \begin{pmatrix} \mathbf{W}^T \\ \mathbf{v}^T \end{pmatrix} \right\|_F^2,$$

with  $\Theta_{\text{in}} = [[\theta^0(0)^T, -1], [\theta^1(0)^T, -1], \dots, [\theta^{n_c}(0)^T, -1]] \in \mathbb{R}^{n_c \times (d+1)}$  is the design matrix with rank  $d+1$ ,  $\Theta_{\text{out}} = [\theta^0(0) - \theta^0(E), \theta^1(0) - \theta^1(E), \dots, \theta^{n_c}(0) - \theta^{n_c}(E)]^T \in \mathbb{R}^{n_c \times d}$  is the response matrix.

We know that

$$\begin{pmatrix} \hat{\mathbf{W}}^T \\ \hat{\mathbf{v}}^T \end{pmatrix} = (\Theta_{\text{in}}^T \Theta_{\text{in}})^{-1} \Theta_{\text{in}}^T \Theta_{\text{out}} \in \mathbb{R}^{(d+1) \times d}. \quad (31)$$

The OLS for each row of  $\mathbf{W}$  and  $\mathbf{v}$  corresponds to the regression model with independent sub-gaussian noise, and then from Theorem 2.2 and Remark 2.3 in [62], we have for each row  $i = 1, \dots, d$

$$\| \hat{\mathbf{W}}[i : ] - \mathbf{W}[i : ] \|_2^2 + (\hat{\mathbf{v}}[i] - \mathbf{v}[i])^2 \leq \text{Var}[\gamma[i]] \frac{d+1 + \log \frac{d}{\delta}}{n_c \lambda_{\min} \left( \frac{\Theta_{\text{in}}^T \Theta_{\text{in}}}{n_c} \right)}, \quad \text{w.p.} \geq 1 - \frac{\delta}{d}, \quad (32)$$

and because of (30) and the fourth assumption, it holds:

$$\|\hat{\mathbf{W}}[i :] - \mathbf{W}[i :] \|_2^2 + (\hat{\mathbf{v}}[i] - \mathbf{v}[i])^2 \leq \eta^2 \sigma^2 E \left[ \frac{m}{b} \right] \frac{d+1 + \log \frac{2d}{\delta}}{n_c \lambda}, \quad \text{w.p.} \geq 1 - \frac{\delta}{d}. \quad (33)$$

We are going now to consider that each row is estimated through a disjoint set of  $n_c$  inspected messages, so that the estimates for each row are independent. We can then apply the union bound and obtain that the Frobenius distance between the two matrices can be bounded as follows:

$$\left\| \begin{pmatrix} \hat{\mathbf{W}}^T \\ \hat{\mathbf{v}}^T \end{pmatrix} - \begin{pmatrix} \mathbf{W}^T \\ \mathbf{v}^T \end{pmatrix} \right\|_F^2 \leq \eta^2 d \sigma^2 E \left[ \frac{m}{b} \right] \frac{d+1 + \ln \frac{2d}{\delta}}{n_c \lambda}, \quad \text{w.p.} \geq 1 - \delta. \quad (34)$$

Now, we study the error of the reconstructed model, given by  $\|\hat{\theta}_c^* - \theta_c^*\|_2$ . Let  $\Delta \mathbf{W} = \hat{\mathbf{W}} - \mathbf{W}$  and  $\Delta \mathbf{v} = \hat{\mathbf{v}} - \mathbf{v}$ . First, we know that

$$\begin{aligned} \hat{\mathbf{W}} \theta_c^* &= (\mathbf{W} + \Delta \mathbf{W}) \theta_c^* = \mathbf{v} + \Delta \mathbf{W} \theta_c^* \\ \hat{\mathbf{W}} \hat{\theta}_c^* &= \hat{\mathbf{v}} = \mathbf{v} + \Delta \mathbf{v}. \end{aligned}$$

Thus, we have

$$\begin{aligned} \theta_c^* - \hat{\theta}_c^* &= \hat{\mathbf{W}}^{-1} (\Delta \mathbf{W} \theta_c^* - \Delta \mathbf{v}) \\ \|\theta_c^* - \hat{\theta}_c^*\|_2 &\leq \left\| \hat{\mathbf{W}}^{-1} \right\|_2 (\|\Delta \mathbf{W}\|_2 \|\theta_c^*\|_2 + \|\Delta \mathbf{v}\|_2) \end{aligned} \quad (35)$$

Take  $n_c$  large enough that the right hand side of (34) is smaller than  $\frac{1}{4} \left( \|\mathbf{W}^{-1}\|_2^2 \right)^{-1} = \frac{\lambda_{\min}^2(\mathbf{W})}{4}$ , then it holds

$$\|\hat{\mathbf{W}} - \mathbf{W}\|_2 \leq \|\hat{\mathbf{W}} - \mathbf{W}\|_F \leq \left\| \begin{pmatrix} \hat{\mathbf{W}}^T \\ \hat{\mathbf{v}}^T \end{pmatrix} - \begin{pmatrix} \mathbf{W}^T \\ \mathbf{v}^T \end{pmatrix} \right\|_F \leq \frac{1}{2} \|\mathbf{W}^{-1}\|_2 \quad \text{w.p.} \geq 1 - \delta$$

then  $\hat{\mathbf{W}}$  is invertible [63, Ch. III, Thm. 7]. Moreover if  $\mathbf{W}$  and  $\mathbf{W} + \Delta \mathbf{W}$  are invertible, then  $(\mathbf{W} + \Delta \mathbf{W})^{-1} = \mathbf{W}^{-1} - \mathbf{W}^{-1} \Delta \mathbf{W} (\mathbf{W} + \Delta \mathbf{W})^{-1}$  and

$$\left\| \hat{\mathbf{W}}^{-1} \right\|_2 \leq \|\mathbf{W}^{-1}\|_2 + \|\mathbf{W}^{-1}\|_2 \|\mathbf{W} - \hat{\mathbf{W}}\|_2 \left\| \hat{\mathbf{W}}^{-1} \right\|_2,$$

From which we derive

$$\left\| \hat{\mathbf{W}}^{-1} \right\|_2 \leq \frac{\|\mathbf{W}^{-1}\|_2}{1 - \|\mathbf{W} - \hat{\mathbf{W}}\|_2 \|\mathbf{W}^{-1}\|_2} \leq 2 \|\mathbf{W}^{-1}\|_2. \quad (36)$$

Finally, from (35), (36), and (34)

$$\begin{aligned} \|\theta_c^* - \hat{\theta}_c^*\|_2 &\leq \left\| \hat{\mathbf{W}}^{-1} \right\|_2 (\|\Delta \mathbf{W}\|_2 \|\theta_c^*\|_2 + \|\Delta \mathbf{v}\|_2) \\ &\leq 2 \|\mathbf{W}^{-1}\|_2 (\|\Delta \mathbf{W}\|_2 \|\theta_c^*\|_2 + \|\Delta \mathbf{v}\|_2) \\ &\leq 2 \|\mathbf{W}^{-1}\|_2 \left( \left\| \begin{pmatrix} \hat{\mathbf{W}}^T \\ \hat{\mathbf{v}}^T \end{pmatrix} - \begin{pmatrix} \mathbf{W}^T \\ \mathbf{v}^T \end{pmatrix} \right\|_F \|\theta_c^*\|_2 + \left\| \begin{pmatrix} \hat{\mathbf{W}}^T \\ \hat{\mathbf{v}}^T \end{pmatrix} - \begin{pmatrix} \mathbf{W}^T \\ \mathbf{v}^T \end{pmatrix} \right\|_F \right) \\ &\leq \frac{2}{\lambda_{\min}(\mathbf{W})} (\|\theta_c^*\|_2 + 1) \times \sqrt{\eta^2 d \sigma^2 E \left[ \frac{m}{b} \right] \frac{d+1 + \ln \frac{2}{\delta}}{n_c \cdot \lambda}}, \quad \text{w.p.} \geq 1 - \delta. \end{aligned}$$

Finally, we observe that the procedure described above considers in total  $d \cdot n_c$  inspected messages. If  $n_c$  denotes the total number of inspected messages, we need to replace  $n_c$  in the formula above by  $n_c/d$ . Since solving a least squares problem with  $m$  points and  $d+1$  variables requires  $O(md^2)$  operations, solving  $d$  least squares problems requires  $O(md^3)$  operations. Replacing  $m$  by  $n_c/d$ , we have the total complexity of computation equal to  $O(n_c d^2)$ .  $\square$

**About the Eigenvalues of the Matrix  $\mathbf{W}$ .**

$\mathbf{H} = \mathbf{x}_c^T x$  is diagonalizable, i.e.,  $\mathbf{H} = \mathbf{U}\Lambda\mathbf{U}^T$  with  $\mathbf{U}$  an orthonormal matrix and  $\Lambda$  a diagonal one. After some calculations

$$\begin{aligned}\mathbf{W} &= I - \left( I - \frac{2\eta}{m} \mathbf{H} \right)^{E\left[\frac{m}{b}\right]} \\ &= \mathbf{U} \left( I - \left( I - \frac{2\eta}{m} \Lambda \right)^{E\left[\frac{m}{b}\right]} \right) \mathbf{U}^T.\end{aligned}$$

Then

$$\begin{aligned}\lambda_{\min}(\mathbf{W}) &= 1 - \left( 1 - \frac{2\eta}{m} \lambda_{\min}(\mathbf{H}) \right)^{E\left[\frac{m}{b}\right]} \\ \lambda_{\max}(\mathbf{W}) &= 1 - \left( 1 - \frac{2\eta}{m} \lambda_{\max}(\mathbf{H}) \right)^{E\left[\frac{m}{b}\right]}\end{aligned}$$

## C Datasets, model, and experimental setup

In this section, we provide supplementary details on the datasets and model (Sec. C.1), and on our experimental setup (Sec. C.2).

### C.1 Datasets and model

**Flight Prices dataset** This dataset contains booking details like origin, destination, booking time before departure, departure date, journey type (round trip or not), airline codes, and segment price, which corresponds to the target in the considered regression task. Similar datasets [64] have been used to model traveller preferences and their price elasticity. The data is split according to airlines resulting in 10 clients. The number of features in this dataset is 9. To show the dissimilarity between the clients local data distribution, the relative Euclidean distance between each client’s optimal local model and the global model is evaluated [65]. We observe from Table 2 that the local data distribution of clients 0 and 6 are very different from the global distribution. This corresponds to the fact that client 0 is a business fares airline and client 6 is a basic economy fares airline. The local dataset size for each client is also given in Table 2.

Airline ID	0	1	2	3	4	5	6	7	8	9
Local data size	2995	17451	11789	9855	8209	8058	4232	4161	3959	19287
Dissimilarity degree	23%	8%	4%	21%	8%	4%	25%	8%	5%	6%

Table 2: Statistics of Flight Prices dataset for every airline. Total size: 100 000 records.

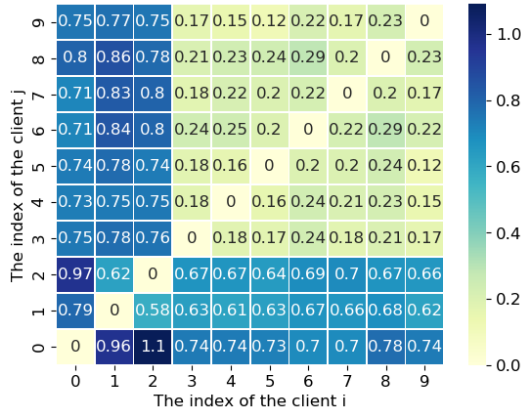


Figure 5: Adult: Clients model heterogeneity,  $\frac{\|\theta_i^* - \theta_j^*\|_2}{\|\theta_j^*\|_2}$

Client ID	0	1	2	3	4	5	6	7	8	9
Local data size	2%	3%	2%	13%	13%	13%	13%	13%	14%	14%

Table 3: Local data size proportion of each client in Adult dataset. Total size: 12 300 records.

**Adult [44]** This dataset contains individual information such as sex, age, education level, family situation, and working class. This information is used to predict whether a person has an income higher than 50k\$. There are 10 clients. To simulate a non-iid data distribution scenario, we distribute the records of people with a PhD degree among the first three clients according to their age. The first client owns the data of young PhDs less than 38 years old, the second client owns the data of PhDs aging between 38 and 52 years old, and the third client owns the data of PhDs elder than 52 years old. The rest of the data is uniformly distributed among the remaining clients. To show the dissimilarity between clients, the relative Euclidean distance between each client’s optimal local

model is evaluated (see Figure 5). We can observe that, due to our specific non-iid data distribution, the optimal local models of the first three clients are quite far from the rest of the optimal local models, which is reasonable as people with PhD degree are more likely to have a different salary prediction pattern. The number of the features in this dataset is 53 and the local dataset size of each client is given in Table 3.

**Leaf Synthetic [45]** This dataset is designed for a classification task, for which clients’ data sets are highly heterogeneous both in terms of number of samples and of underlying statistical distribution.<sup>11</sup> The detailed generation procedure can be found in [45, Appendix A]. The number of features in this dataset is set to 100. The number of the clients is set to 10. To simulate a non-iid distribution across clients, the number of clusters is set to 5. The local dataset size is the same for all clients and equals to 2000.

**AT&T [19]** This dataset contains a set of facial images from 40 people. The database was used in the context of a face recognition project carried out in collaboration with the Speech, Vision and Robotics Group of the Cambridge University Engineering Department.

There are ten different images of each of 40 people. For some people, the images were taken at different times, varying the lighting, facial expressions (open / closed eyes, smiling / not smiling) and facial details (glasses / no glasses). All the images were taken against a dark homogeneous background with the people in an upright, frontal position (with tolerance for some side movement). The size of each image is 70x80 pixels, with 256 grey levels per pixel. There are 10 clients involved in the FL training. Each client has all the images of 4 randomly chosen people and only a subset of facial images (of size 3 or 4) of the remaining people. The local dataset size for each client is given in Table 4.

Client ID	0	1	2	3	4	5	6	7	8	9
Local data size	12%	12%	12%	12%	8%	8%	8%	8%	8%	12%

Table 4: Local data size proportion of each client in AT&T dataset. Total size: 1800 records.

**Model** For Figlit Prices, Adult and Leaf Synthetic dataset, the model is a neural network with 3 hidden layers, that each has 256 neurons followed by an ReLU activation layer. For AT&T, to have a comparable model size with the other datasets, the training model is shrank to a neural network with 3 hidden layers, that each has 32 neurons followed by an ReLU activation layer.

In [10], the authors claim that using batch normalization [66] in a neural network but not sharing the BatchNorm statistics of the private batch between the server and the clients [36], can weaken the attack performance in FL. Thus, the clients train also the above mentioned neural network with an extra BN layer added in front of every ReLU activation layer. Again, the corresponding BN statistics during the training are not shared between the clients and the server.

## C.2 Experimental Setup

For all the FL training, the learning rate is set to 1e-2 and the number of communication rounds is set to 1000. The adversary inspects the exchanged message in every 10 communication rounds. Therefore, the size of inspected messages, i.e.,  $|\mathcal{M}_c|$ , is 100.

For the experiments where we vary the client’s local dataset size to different values  $\{d^1, d^2, \dots\}$ : Let  $\{D^1, D^2, \dots\}$  be the set of the corresponding local dataset. To build  $D^1$ , we choose randomly  $d^1$  samples without replacement from the client’s original local dataset  $\mathcal{D}_c$ . Then, to build  $D^i$ , we add additional  $(d^i - d^{i-1})$  samples which are randomly chosen from  $\mathcal{D}_c \setminus D^{i-1}$  into  $D^{i-1}$ .

For the experiments where we vary the number of clients to  $n > |\mathcal{C}|$ : Remind that  $|\mathcal{C}|$  is the default number of clients. For AT&T dataset, we randomly choose  $n - |\mathcal{C}|$  clients with replacement to duplicate. For Leaf Synthetic dataset, we set the number of the clients to  $n$ .

For datasets Flight Prices, Adult, and Leaf Synthetic, the training is done using a NVIDIA T4 GPU (an AWS instance g4dn.xlarge of 8 vCPU, 16 GB system memory). For dataset AT&T, the training

<sup>11</sup>The underlying statistical distribution is determined by the number of clusters.

is done using a NVIDIA T4 GPU (an AWS instance g4dn.8xlarge of 32 vCPU, 128 GB system memory). All our experiments are implemented using PyTorch. The additional experimental settings for the attacks are given below.

**Local model reconstruction attack** Tables 5, 6, 7, and 8 give the details on hyper-parameters used in our heuristic (Algorithm 2) including the training of mapping function (Eq. 7) and the training of local update difference (Eq. 8) on Flight Prices, Adult, Leaf Synthetic, and AT&T datasets, respectively. The notation  $A \times B$  presents a neural network with  $B$  hidden layers of  $A$  neurons each followed by one ReLU activation layer.

Eq. 7	client ID	0	1	2	3	4	5	6	7	8	9
	Architecture	64x2									
	Learning rate	1e-5	1e-5	1e-5	1e-6	1e-5	1e-5	1e-5	1e-5	1e-4	1e-6
Eq. 8	client ID	0	1	2	3	4	5	6	7	8	9
	Epochs	1e4	7e3	1e4	6e3						
	Learning rate	1e-3	1e-2	1e-3	1e-3	1e-2	1e-2	1e-2	5e-3	1e-3	1e-3

Table 5: Hyper-parameters used in local model reconstruction attack on Flight Prices dataset.

Eq. 7	client ID	0	1	2	3	4	5	6	7	8	9
	Architecture	16x2	16x2	32x2	32x2	32x2	32x2	32x2	16x2	16x2	16x2
	Learning rate	1e-3	1e-3	1e-5	1e-4						
Eq. 8	client ID	0	1	2	3	4	5	6	7	8	9
	Epochs	1e3	1e3	1e3	1e3	1e3	1e3	1e2	1e3	1e3	1e3
	Learning rate	1e-1	1e-2	1e-1	1e-1	1e-2	1e-1	1e-2	1e-1	1e-1	1e-1

Table 6: Hyper-parameters used in local model reconstruction attack on Adult dataset.

Eq. 7	client ID	0	1	2	3	4	5	6	7	8	9
	Architecture	32x2									
	Learning rate	1e-4	1e-4	1e-4	1e-4	1e-4	1e-3	1e-4	1e-4	1e-4	1e-4
Eq. 8	client ID	0	1	2	3	4	5	6	7	8	9
	Epochs	5e3									
	Learning rate	1e-2									

Table 7: Hyper-parameters used in local model reconstruction attack on Leaf Synthetic dataset.

Eq. 7	client ID	0	1	2	3	4	5	6	7	8	9
	Architecture	64x2									
	Learning rate	1e-4									
Eq. 8	client ID	0	1	2	3	4	5	6	7	8	9
	Epochs	1e4									
	Learning rate	1e-3									

Table 8: Hyper-parameters used in local model reconstruction attack on AT&T dataset.

**Attribute inference attack** For the baseline [11], which aims to solve the Problem (2), we use an LBFGS optimizer with learning rate 1e-3, 1e-2, and 5e-3 for Flight Prices, Adult, and Leaf Synthetic datasets, respectively.

**Sample reconstruction attack** For the baseline [7] which aims to solve the Problem (4), we use an SGD optimizer with learning rate 1e-3.

For the model-based attacks, which aim to solve the Problem (5), we use an SGD optimizer with learning rate 1e-3, 1e-4 and 1e-4 for the attack triggered on the local model reconstructed from LMRA, the global model, and the last-returned model, respectively.

**Source inference attack** For the baseline [16], it happens that the source may be different at different round, while [16] does not provide a way to determine a final answer. In our experiment, to make their attack complete, we choose the client who has been selected the most as source, i.e.,  $\operatorname{argmax}_{c' \in \mathcal{C}} |\{t | c' = \operatorname{argmin}_{c \in \mathcal{C}} l(\theta_c(t), \mathbf{x}_c, y), \forall t \in \{0, \dots, T-1\}\}|$ .

## D Additional experimental results

### D.1 Model performance

In Table 9, we show the average training performance of the global model, the last-returned model, and our reconstructed model (considered in Table 1) on the client’s local dataset, as well as the average training performance of the optimal local model. The model performance is quantified by the mean absolute percentage error (MAPE)<sup>12</sup> for regression tasks (Flight Prices dataset), and by the model accuracy for classification tasks (Adult, Leaf Synthetic, and AT&T datasets).

Metric	Dataset	Without BN				With BN			
		Global	Last-returned	Ours	Optimal local	Global	Last-returned	Ours	Optimal local
MAPE	Flight Prices	16.4	16.9	13.3	<b>10.7</b>	16.2	15.9	13.9	<b>10.3</b>
	Adult	74.4	73.9	79.6	<b>90.5</b>	72.1	72.7	77.6	<b>90.1</b>
Accuracy	Leaf Synthetic	77.0	75.1	83.8	<b>89.9</b>	74.2	72.6	80.0	<b>88.6</b>
	AT&T	74.3	75.2	87.7	<b>88.5</b>	70.1	71.3	86.8	<b>87.9</b>

Table 9: The training performance of the models (considered in Table 1) and of the optimal local model, when training a neural network w/wo batch normalization (BN) with 1 local epoch and batch size 512 (32 for AT&T dataset).

From Table 9, we can see that our local model reconstructed by LMRA overfits more the client’s local data than the global model and the last-returned model.

<sup>12</sup>MAPE(y,  $\hat{y}$ ) =  $\frac{1}{N} \sum_{i=0}^{N-1} \frac{|y_i - \hat{y}_i|}{y_i}$  where y is the ground truth target value,  $\hat{y}$  is the prediction and N represents the number of samples)

## D.2 Examples of images recovered from SRA when training with batch size 64

Here we show the examples of images recovered from SRA when training a fully-connected 3-layer neural network without batch normalization on AT&T dataset among 10 clients through FedAvg under batch size 64 and 1 local epoch. Images (b), (c), and (d) are reconstructed by the model-based SRA [12] on the reconstructed model from LMRA, the last-returned model, and the global model, respectively. Image (e) is obtained by the well-known gradient-based SRA [7] (Problem (4)).



### D.3 Impact of batch size and of the number of local epochs on LMRA, AIA, and SIA

Here, we investigate the sensitivity of the LMRA, AIA, and SIA on the batch size (Figure 6) and on the number of local epochs (Figure 7). For Flight Prices, Adult, and Leaf Synthetic, default values for the number of local epochs and the batch size are 1 and 512, respectively. For AT&T, default values for the number of local epochs and the batch size are 1 and 32, respectively.

**Impact of batch size** For LMRA, our attack performance (measured by the model similarity to the optimal local model [51]) improves when the batch size increases. Since large batch sizes introduce less randomness in pseudogradients, they lead to a more accurate estimation of  $\mathcal{G}_c$ , and, consequently, to a more accurate reconstructed model (see discussion in Sec. 3.2). For the SOTA AIA, since the virtual gradient is computed based on the whole local dataset of client  $c$  (Problem (2)), when the batch size is larger, the pseudogradient  $\theta(t) - \theta_c(t)$  is closer to the virtual one. Therefore, as expected, we observe that AIA performance increases as the batch size increases. Overall, our LMRA-based AIA and SIA outperform the SOTA attacks in all the settings except for SIA on Leaf Synthetic with batch size 128.

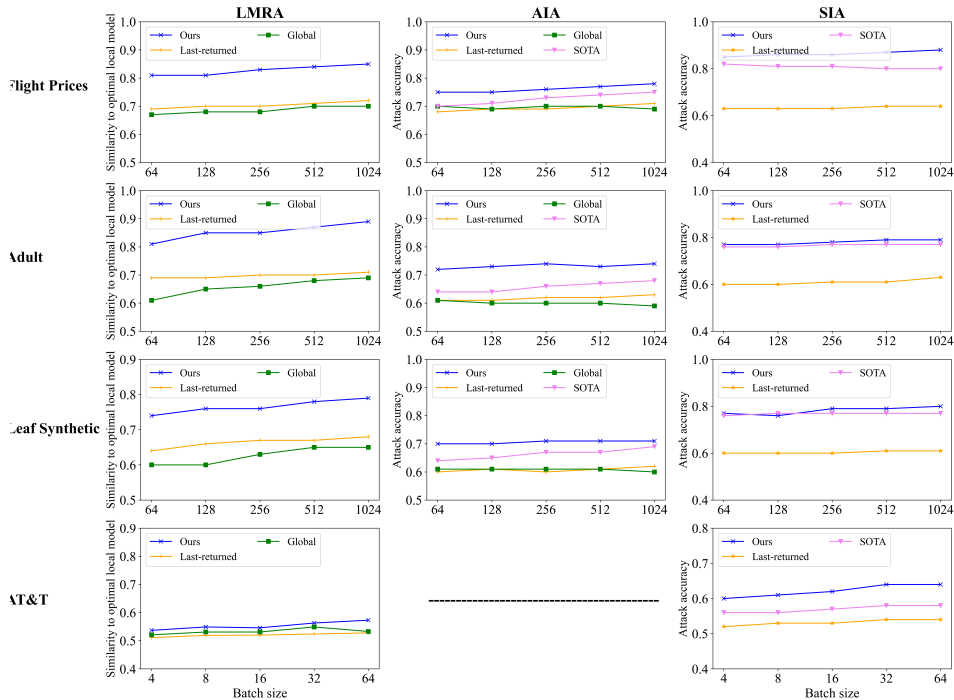


Figure 6: Batch size effect on LMRA, AIA, and SIA when training a neural network wo BN. Default value for the number of local epochs is 1.

**Impact of the number of local epochs** Compared with the SOTA AIA, our LMRA-based AIA is much less sensitive to the number of local epochs. When the number of local epochs increases from 1 to 10, our LMRA-based AIA performance is maintained or even improves, whereas the SOTA AIA performance drops significantly. For model-based SIAs (ours and the SOTA attack), the performances are insensitive to the number of local epochs. Overall, our LMRA-based attacks outperforms the SOTA attacks in all the configurations.

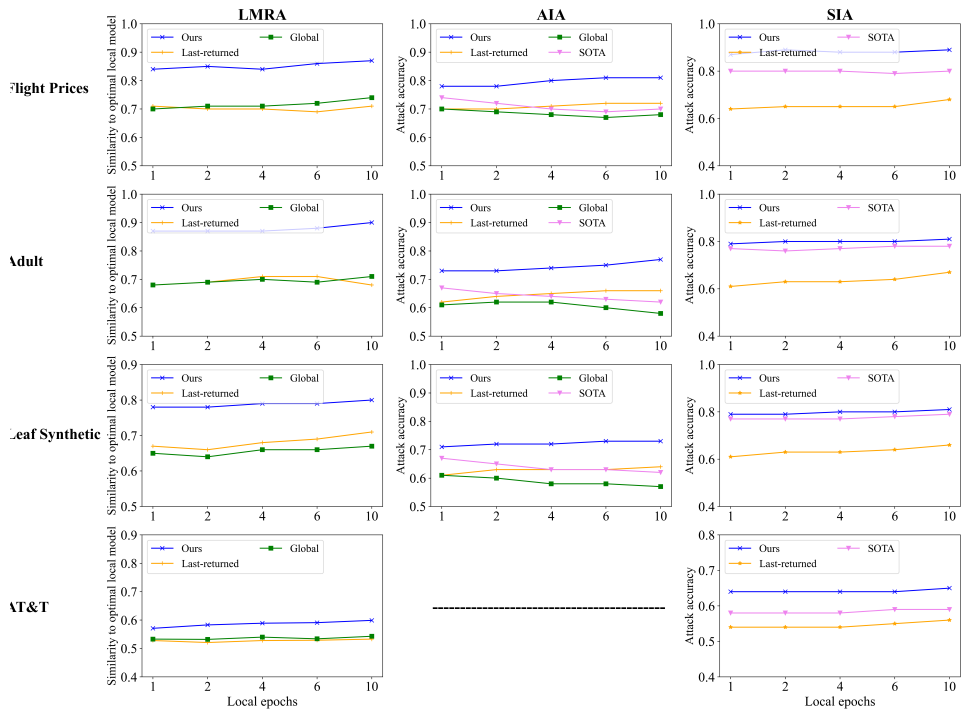


Figure 7: The number of local epochs effect on LMRA, AIA, and SIA when training a neural network wo BN. Default value for the batch size is 512 for Flight Prices, Adult, and Leaf Synthetic and 32 for AT&T.

#### D.4 The performance of attacks under defenses

To mitigate the privacy leakage, we have tested three defenses. The first one, referred to as DP, is to extend DPSGD algorithm [37] that clips and adds Gaussian noises to the client’s gradients in FL. The corresponding method provides theoretical guarantees on the privacy budget  $(\epsilon, \delta)$  in sample-level differential privacy [54, 67]. We used Opacus [68] to incorporate a  $(10, 10^{-5})$ -differentially private defense. The second one, referred to as Mixup, is to train a model on composite data samples by a linear combination of sample pairs [40], e.g., an average one in our implementation. Mixup was proposed to improve the generalization of ML model and recent work [69] shows that it can defend against adversarial attacks. The third one, referred to as DP+Mixup, is a direct combination of the two above mechanisms. The results are given in Table 10.

Dataset	Method	LMRA		AIA		SIA		SRA	
		Ours	Global	Ours	SOTA	Ours	SOTA	Ours	SOTA
Flight Prices	No defense	84.2	71.4	<b>77.2</b>	73.1	<b>84.3</b>	82.1	-	-
	DP	71.4	59.6	<b>71.3</b>	66.6	<b>76.6</b>	72.1	-	-
	mixup	80.3	68.2	<b>75.1</b>	72.3	<b>82.0</b>	80.6	-	-
	DP + mixup	64.6	57.4	<b>68.6</b>	65.9	<b>75.2</b>	72.6	-	-
Adult	No defense	88.4	70.7	<b>73.1</b>	67.6	<b>78.6</b>	75.1	-	-
	DP	79.6	61.9	<b>68.6</b>	62.5	<b>73.5</b>	73.1	-	-
	mixup	86.3	68.8	<b>72.1</b>	66.4	<b>77.0</b>	73.6	-	-
	DP + mixup	77.3	60.3	<b>66.0</b>	61.7	<b>71.9</b>	71.2	-	-
Leaf Synthetic	No defense	78.2	67.3	<b>71.1</b>	66.3	<b>77.9</b>	74.6	-	-
	DP	72.1	60.4	<b>63.3</b>	61.1	<b>71.2</b>	70.8	-	-
	mixup	76.3	63.0	<b>69.9</b>	65.1	<b>74.5</b>	71.6	-	-
	DP + mixup	71.8	60.1	<b>62.5</b>	60.8	<b>70.2</b>	69.9	-	-
AT&T	No defense	57.3	52.8	-	-	<b>61.6</b>	57.1	<b>34.3</b>	26.1
	DP	52.1	48.4	-	-	<b>57.6</b>	52.4	<b>23.4</b>	18.7
	mixup	54.1	50.4	-	-	<b>60.3</b>	56.1	<b>33.7</b>	25.1
	DP + mixup	50.1	49.6	-	-	<b>55.0</b>	51.4	<b>23.1</b>	18.0

Table 10: LMRA, AIA, SIA, and SRA’s performance under three defenses when training a neural network without batch normalization with 1 local epoch and batch size 512 (32 for AT&T dataset).